Politecnico di Torino

Corso di Laurea Magistrale in Ingegneria Energetica e Nucleare
A.a. 2020/2021
Sessione di Laurea ottobre 2021

Experimental characterization of a pre-commercial Anion Exchange Membrane electrolyzer and its techno-economic prospects for industrial-scale hydrogen production

Relatori:

    prof. ANDREA LANZINI
    prof. MASSIMO SANTARELLI

Tutor Aziendale Edison Spa:

    dott. MASSIMILIANO BINDI

Candidato:

    ROBERTA BIGA

Acknowledgements

Abstract

As more countries pursue deep decarbonization strategies, hydrogen will have a critical role to play. This will be particularly so in harder-to-abate sectors, such as steel, chemicals, long-haul transport, shipping and aviation. In this context, hydrogen needs to be low carbon from the outset and ultimately.

In recent years, research has been focusing on the development of technologies for green hydrogen production, but the cost of production is a barrier to the uptake of green hydrogen.

Among the technologies available or under development, electrolysis from renewable sources is attracting lot of interest. In this scenario, the thesis project, developed in collaboration with Edison S.p.a, is born.

The thesis is divided into two sections: in the first place it is performed an experimental assessment of a pre-commercial device based on AEM technology, located in the laboratory of 'Officine Edison Torino'; secondly, the modelling and simulation of a 'power -to - hydrogen' system, using the real data of the AEM electrolyzer previously studied, is developed within the MATLAB environment.

The first part aims to investigate the performances of the electrolyzer varying some operating conditions: the hydrogen flow rate production, the hydrogen production pressure, and the electrolytic solution temperature. In addition, the working point where the stack efficiency reaches its maximum value is identified.

Firstly, within the limits of data confidentiality, the test bench and the main components of the device are described. Then, the carried-out experimental tests are explained, and the main results are shown: the stack efficiency varies mainly with the production level, while it is less affected by the hydrogen pressure and cell temperature. Furthermore, the highest stack efficiency, corresponding to 58.8%, is reached at a current density of 0.4 A/cm2 and a hydrogen production pressure of 1 bar.

Finally, some results' comments together with the experimental limitations are reported.

Considering the second section, it is carried out a techno-economic analysis on a system producing hydrogen from a photovoltaic field without the power grid support. The hydrogen is then supplied in a blending with natural gas to an industrial plant, thus allowing partial decarbonization of its production.

The objective is to opportunely size the main system components in order to satisfy the hydrogen request all year while keeping as low as possible the Levelized Cost of Hydrogen.

In the thesis, first of all, the main system's components and the assumptions done are shown and the implemented sizing strategy is explained. Afterward, the Levelized cost of hydrogen produced by the off-grid system is calculated to be equal to 15€/kgH2. Furthermore, a sensitivity analysis on the LCOH varying some characteristics of the AEM electrolyzer is carried out. Considering both stack efficiency and investment cost equal to the 2050 FCH JU targets, it is obtained that the LCOH decreases until the value of 8.7 €/kgH2.

Finally, a techno-economic comparison between the off-grid configuration and grid-connected systems is carried out. The system, provided with the electrolyzer power supply from both photovoltaic field and electric grid, is the most economically favourable, with a LCOH equal to 7.24 €/kgH2.

Contents

List of figures

List of tables

1. Introduction

The world faces a major challenge to avoid climate catastrophe. The only possible path is to decarbonize the global economy, achieving "net zero" emissions around 2050 [1].

Italy is expected to achieve the 95% decarbonization target by 2050 and therefore, the emissions reduction project needs to substantially accelerate [1]. In this scenario, green hydrogen plays an important role, first because it's a carbon-neutral gas and can significantly contribute to the decarbonization of the so-called "hard-to-abate" sectors, and second because it can become cost-competitive [1].

Green hydrogen can be used across many different sectors [2]:

- Transport sector: it can be used as fuel in fuel cell electric vehicles. Especially, hydrogen trains are already a cost-effective option to replace diesel trains, and long-haul trucks and buses are expected to become cost-competitive by 2030. Instead, regarding cars, electrification is expected to be the main option for the decarbonization of vehicles and using hydrogen as a fuel is considered a less favourable path [1].
- Building sector: blending hydrogen with natural gas or combining them to produce synthetic methane and then injecting it into the gas grid, is an efficient way to start the decarbonization of gas heating systems. However, although in theory hydrogen and NG can be mixed in any proportions, the blend should be carefully selected to be compatible with the existing gas equipment [3].
- Industrial sector: hydrogen can be used as feedstock in the chemical industry to the production of ammonia, synthetic fuels and various types of fertilisers. It can be largely used also in the iron and steel subsectors. In addition, hydrogen is considered one of the few options to decarbonize industries using high-temperature processes, as furnaces [1].

Furthermore, hydrogen can help balance fluctuations of the grid: renewable power overproduction in summer can be converted into hydrogen and stored for the winter months [1].

In addition, it can be used to transport renewable energy from a place of high availability of natural resources and low request to a place with high demand but low energy production. The produced hydrogen is then transported through the existing gas infrastructures.

In this scenario, Edison decides to investigate an emerging technology for hydrogen production from renewable sources. Especially, the company wants to conduct an experimental analysis on a small-scale pre-commercial anion exchange membrane (AEM) electrolyzer.

The aim of this project is to understand the actual technological level of the AEM electrolysis system and to acquire knowledge of its operating modes. Therefore, obtaining an overall assessment of the product by

considering also the economic aspects, its insertion as a possible solution for future industrial projects of Edison may be considered.

In this work, after a brief summary on the methods of producing hydrogen from renewable sources, the emerging AEM electrolysis technology will be analyzed in more detail.

Subsequently, a techno-economic analysis of the application of this electrolysis system within a power-to-hydrogen scenario will be carried out.

2. Green hydrogen production

Hydrogen is one of the most abundant elements available on our planet and, in particular, it is contained in water and in hydrocarbons. However, it is not available as a free chemical element, and therefore, it must be produced.

It can be obtained from a variety of methods, but by far the most common is steam reforming of methane or other hydrocarbons which, however, causes significant emissions [4].

In recent years many efforts have been built on technologies to produce green hydrogen.

At present, water electrolysis and steam reforming of biomethane/biogas with or without carbon capture are the most established technologies [5].

Less mature pathways are biomass gasification and pyrolysis, supercritical water gasification of biomass and combined anaerobic digestion and dark fermentation [5].

Research is also focusing on emerging water-splitting technologies, such as photoelectrochemical, thermochemical cycles, photobiological, photocatalysis [5].

Among all the hydrogen production technologies, only water electrolysis powered by renewable energy is further investigated in this thesis.

2.1 Water electrolysis

Water electrolysis consists in the conversion of water into hydrogen, by using electricity available from renewable energy sources [6]. Due to both the low-cost electricity source and manufacturing advancements that have shown early feasibility, this technology is promising to become economical competitive with fossil fuel–derived hydrogen [7].

Two main groups of electrolysis' technologies can be distinguished depending on the process temperature: low temperature and high temperature electrolysis. The former is already well developed and cost-competitive, while the latter is not currently mature enough to address the actual markets, but it may have applicability in the future [7].

Low temperature electrolysis is characterized by cell temperatures around 40-80 °C and it includes alkaline water electrolysis (ALK), proton exchange membrane electrolysis (PEM) and anion exchange membrane electrolysis (AEM). All of these technologies have opportunities to further cost reduction and efficiency improvements, even the ALK and PEM electrolyzers which have been commercially available for many years [7].

Alkaline water electrolyzers and proton exchange membrane water electrolyzers are already commercially available technologies, while anion exchange membrane-based systems still need development to reach acceptable durability and performance levels and therefore, many research activities are focusing on it [7].

High temperature electrolysis, instead, is characterized by much higher operation temperatures, around 700-900 °C, and it includes solid oxide electrolysis (SOEC). It is a less mature technology, and its investment costs are still very high. However, SOEC is expected to have a greater efficiency compared to low temperature electrolyzers [5].
Because of the high working temperature, high temperature electrolysis needs for high-temperature sources of heat close, like concentrated solar power or high temperature geothermal. This might limit the long-term viability of SOEC [5].

As regards the electrolytic process, the reaction takes place in a unit called electrolyzer.
It consists of 2 electrodes, an anode and a cathode, where respectively the oxygen evolution reaction (OER) and the hydrogen evolution reaction (HER) occur, separated by an electrolyte, which can be solid or liquid. Depending on the type of the involved electrolyte material and therefore on the ionic species it is able to conduct, different reactions will occur at the anode and cathode side and consequently different type of electrolysis can be distinguished. [8].
The following chapters will further focus on low-temperature water electrolysis technologies: the already well-established alkaline electrolysis (ALK) and proton exchange membrane electrolysis (PEM), and the emerging one, the anion exchange membrane electrolysis (AEM).

2.1.1   Technologies overview

2.1.1.1   Alkaline electrolysis

Hydrogen production by alkaline water electrolysis is a well-established technology up to the megawatt range and it represents the most widely used electrolytic technology on a commercial level worldwide [4].

In the ALK cell, the two electrodes are immersed in a liquid electrolyte, which is typically an aqueous solution of potassium hydroxide (KOH) with 20 to 30 wt. % KOH [9]. The most commonly used anode and cathode materials are respectively nickel- and cobalt-based oxides [6].

The two electrodes are separated by a porous diaphragm. It is typically made of ceramic oxides such as asbestos and potassium titane or polymers such as polypropylene and polyphenylene sulfide [6]. The role of the diaphragm is to separate the produced gases from their respective electrodes and avoiding safety issues due to the mixing of the produced gases [10].

In Figure 1 the electrolytic process is represented and the equations 1-3 show the chemical reactions which occur respectively at the cathode and anode side and the overall reaction.
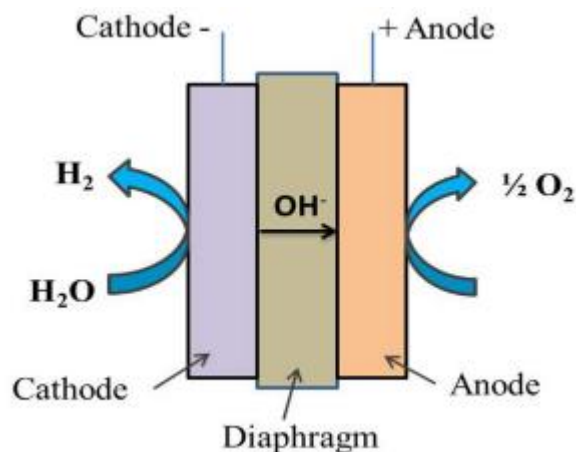
Figure 1 - schematic illustration of alkaline water electrolysis [10]

Cathode $$2H_2O_{(l)} + 2e^- \rightarrow H_{2(g)} + 2OH^-_{(aq)}$$ (1)

Anode: $$2OH^-_{(aq)} \rightarrow \tfrac{1}{2} O_{2(g)} + H_2O_{(l)} + 2e^-$$ (2)

Overall reaction: $$H_2O_{(l)} \rightarrow H_{2(g)} + \tfrac{1}{2} O_{2(g)}$$ (3)
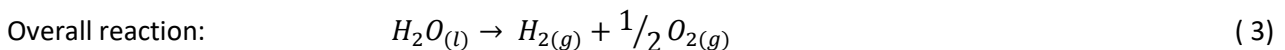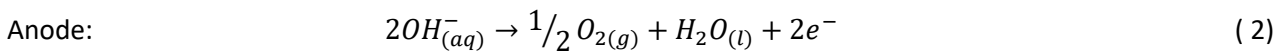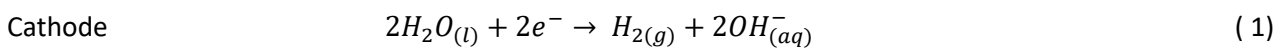
At the cathode side the reduction reaction occurs, and two molecules of water are split into one molecule of hydrogen and two hydroxyl ions. The negative ions diffuse through the porous diaphragm to the anode, where an oxidation reaction takes place: ½ molecule of oxygen and one molecule of water are produced, and two electrons are delivered.

Proton exchange membrane electrolysis

Proton exchange membrane (PEM) water electrolysis is a young technology that show good performance and stability and it's increasingly establishing itself on the market place [4].

In PEM electrolysis, very expensive electrocatalysts are needed and typically, the anode and cathode catalysts are IrO2 and Pt black, respectively [6].
 Furthermore, an acid membrane is used as solid electrolyte, instead of a liquid electrolyte. The membrane is made of polysulfonate, typically *Nafion*. It has a double function, it conducts H$^+$ ions from anode to cathode and it separates hydrogen and oxygen that are produced in the reaction. [6]
The hydrogen production mechanism occurring inside a PEM cell is shown in Figure 2 and the equations 4-6 report the driven chemical reactions.
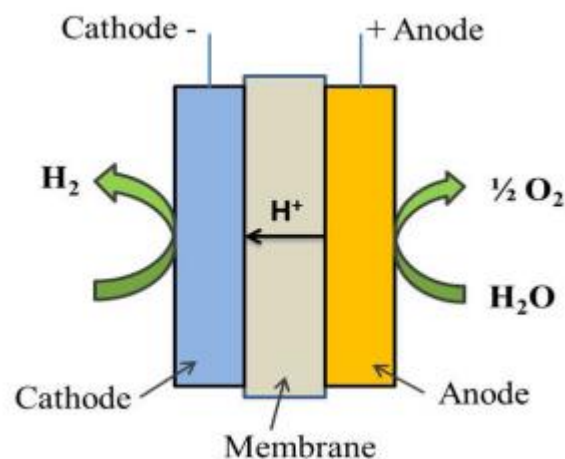
Figure 2 - Schematic illustration of PEM water electrolysis [10]

Cathode: $$2H^+ + 2e^- \rightarrow H_{2(g)}$$ (4)

Anode: $$H_2O_{(l)} \rightarrow 2H^+ + \frac{1}{2}O_{2(g)} + 2e^-$$ (5)

Overall reaction: $$H_2O_{(l)} \rightarrow H_{2(g)} + \frac{1}{2}O_{2(g)}$$ (6)
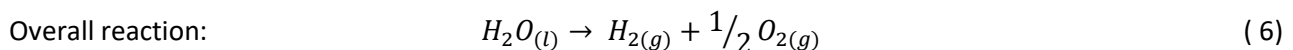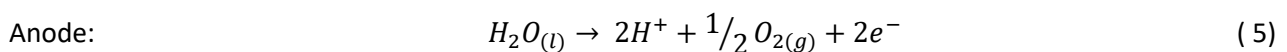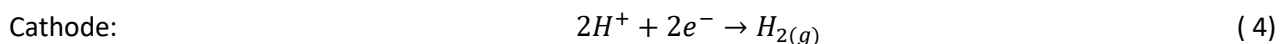
Unlike the alkaline technology, the water is pumped to the anode side. Here the oxidation reaction occurs and, for each molecule of water, ½ molecule of gaseous oxygen is produced and 2 protons and 2 electrons are delivered. The protons diffuse through the membrane to the cathode side, while the electrons arrive to the cathode side through an external power circuit. Finally, at the cathode the protons are reduced producing hydrogen.

2.1.1.3   Anion exchange membrane electrolysis

Anion exchange membrane (AEM) electrolysis is a developing technology and research has been boosted recently in this area [4].

The anode and the cathode are separated by a solid membrane whose function is to transport hydroxyl ions from cathode to anode and to act as a barrier from electrons and gases produced during the reactions [6]. It is composed of a polymer backbone coupled with anion exchange functional group, typically quaternary ammonium ion-exchange group. The polymer matrix is responsible for mechanical and thermal stability, while the functional group is responsible for the ion exchange capacity and ionic conductivity [6].

The AEM has a lower conductivity than PEM, mainly because of the lower mobility of hydroxyl ions compared to protons. Therefore, polymers with higher ion exchange capacity are usually used, which then typically take up more water and have reduced mechanical robustness under flooded conditions [7].

Furthermore, the ability to perform electrochemical compression in the stack is an advantage compared to ALK systems, but this causes poor membrane strength [7].

Therefore, the membrane properties still need to be optimized.

Both the oxygen evolution reaction (OER) and the hydrogen evolution reaction (HER) need electrocatalysts to overcome the kinetics of the reaction. To reduce the investment cost, the development of non-noble metal catalysts is crucial and thus many studies are dealing with this field [6].

Currently, the most used OER catalysts are IrO2, Ni, Ni-Fe alloys, graphene, $Pb_2Ru_2O_{6.5}$, and $Cu_{0.7}Co_{2.3}O_4$, while Pt-black, $CuCoO_x$, Ni-Mo, Ni/CeO_2-La_2O_3/C, Ni, and graphene are used as HER catalysts [6].

Regarding the electrolytic solution, typically, a small percentage of electrolyte (HCO_3^-/CO_3^{2-} or dilute KOH) is added to the water feed, in order to increase the cell performance. AEM electrolyzers can operate with water feed at both electrodes or in anode feed only [4]. However, the water electrolyte, generally, only circulates in the anode half-cell and the cathode side remains dry, to reduce the moisture content in the produced hydrogen [11] and to increase the cell stability [7]. Therefore, the water management in AEM cells is more difficult than in PEM cells and it's a cause of performance reduction: the water is supplied to the cathode by water transport through the membrane, which causes mass transport limitations and lowers the maximum achievable current densities [7].

Many studies are now focusing on improving the AEM technology performance, in particular the main issues they're trying to solve are related to the trade-offs between conductivity and mechanical properties of the membrane, to the water management, to the catalyst/electrolyte interactions, and to the durability [7].

The concept of AEM water electrolysis is shown schematically in Figure 3 and the chemistry is expressed through the equations 7-9.
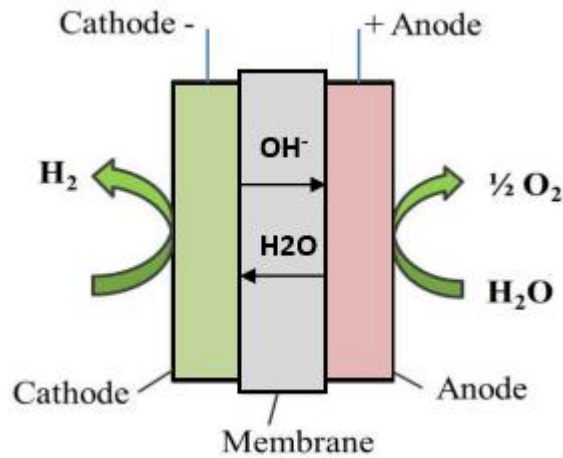
Figure 3 - Schematic illustration of AEM water electrolysis

Cathode

$$2H_2O_{(l)} + 2e^- \rightarrow H_{2(g)} + 2OH^-_{(aq)} \qquad (7)$$

Anode:

$$2OH^-_{(aq)} \rightarrow {}^1\!/_2\,O_{2(g)} + H_2O_{(l)} + 2e^- \qquad (8)$$

Overall reaction:

$$H_2O_{(l)} \rightarrow H_{2(g)} + {}^1\!/_2\,O_{2(g)} \qquad (9)$$
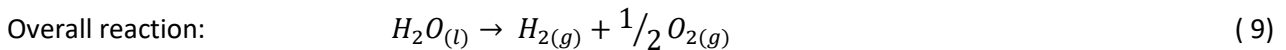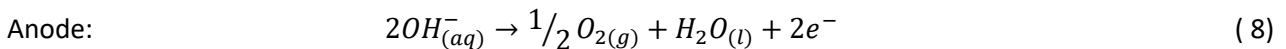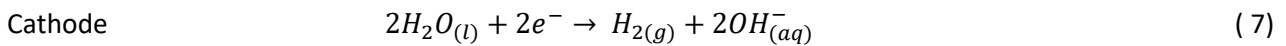
The water is pumped to the anode side and it crosses the membrane to reach the cathode side where it is reduced to form gaseous hydrogen and hydroxyl ions. The latter diffuse through the AEM to the anode section. Here an oxidation reaction occurs and each 2 ions, ½ molecule of hydrogen and 1 molecule of water are produced, and 2 electrons are delivered to the external circuit.

2.1.2   Techno-economic comparison

The three technologies previously described have different technology readiness levels (TRLs).
Alkaline and PEM electrolysis are already well developed, in particular the former has a TRL equal to 9 and it is commercially used in industry, while the latter is mainly used for medium and small applications (TRL = 6 - 8). The AEM technology, instead, is still in development and demonstration (TRL= 5 -6) and it has started to be used in small commercial applications [12].

Also, different KPIs characterize the three types of electrolysis, as it can be noted in Table 1.

AEM electrolysis is a very promising technology since it already shows the highest electrical efficiency and the lowest operating temperature range, even though it is still not mature.

Because of the membrane-type design [13], PEM electrolysis is able to produce hydrogen with a very high level of purity and at a maximum outlet pressure of 80 bar, which could eliminate the need of a compressor stage after the production.

The alkaline technology shows the longest stack lifetime, and this is due also to the already high TRL. Nevertheless, due to the large internal resistance incurred across the diaphragm and liquid electrolyte, AE technology normally operates at low current density (<0.5 A/cm2) [13].

	ALKALINE EL	PEM EL	AEM EL
Electrical system efficiency [%, LHV]	63 - 70	56 - 60	60 - 72
Operating pressure [bar]	1 - 30	30 - 80	1 – 30 [4]
Operating temperature [°C]	60 - 80	50 - 80	20 - 45
Current density [mA/cm2] [6]	200 - 500	800 - 2500	200 - 500
H2 purity [vol%] [6]	99.3 – 99.9	99.9999	99.99
Stack lifetime (operating hours x1000)	60 - 90	30 - 90	40
Degradation (%/1000hrs)	0.13	0.2	>1

Table 1 – KPIs comparison [14]– data are referred to the actual state of art

Finally, looking at the investment costs of the three technologies, the anion exchange membrane cell and the PEM cell are the most expensive, respectively 1200 €/kWe and 900 – 1500 €/kWe [14]- [15] - [16]. The cost of the former is high since it still has a low exploitation degree, while the highest cost of the latter is due to its expensive electrocatalysts. The future cost projections to 2030, indeed, show a decrement of both cost, but the cost of PEM is expected to remain the highest one (AEM: 450 €/kWe, PEM: 500 €/kWe). [14]- [15] - [16]

Regarding the alkaline technology the actual CAPEX is 400 – 1200 €/kWe. It is assumed to decrease in the future to 400 €/kWe [14]- [15] - [16].

Lastly, the main advantages and disadvantages of the three technologies previously described are summarized in Table 2.

	Advantages	Disadvantages
Alkaline EL	Mature technology	Low operating current densities
	No-noble metal catalysts	Low dynamic
	Long term stability	Low operating pressure
	Low cost materials	Corrosive liquid electrolyte
PEM EL	High operating current densities	High cost of materials
	Dynamic operation possible	Noble metal catalysts
	High gas purity	Stack below MW range
	Compact system	
AEM EL	No-noble metal catalysts	Still a developing technology
	Dynamic operation possible	Cell production processes still costly
	Very high native gas purity	Stack below 100kW range

Table 2 – Advantages and disadvantages of alkaline, PEM and AEM electrolysis [[14]+ [6]]

2.1.3 Electrochemistry overview

In water electrolysis, water dissociates into molecular hydrogen and oxygen.

Enthalpy, entropy and Gibbs free energy change are the following [17]:

$$\Delta H°(H_2O_{(l)}) = +285.84 \ ^{kJ}/_{mol}$$

$$\Delta S°(H_2O_{(l)}) = +163.15 \ ^{J}/_{mol*K}$$

$$\Delta G°(H_2O_{(l)}) = \Delta H°(H_2O_{(l)}) - T\Delta S°(H_2O_{(l)}) = +237.22 \ ^{kJ}/_{mol}$$

As the Gibbs free energy change is positive, the reaction is non-spontaneous, and therefore electric energy has to be provided to water to allow the electrolysis to happen.

Theoretically, the minimum cell voltage for water electrolysis operation is the reversible voltage and it is expressed by equation (10), which is called Nernst equation.

$$U_{rev} = \frac{\Delta G}{zF} \qquad (10)$$

Being, z the electrons transferred per reaction, in this case z=2;

    F the Faraday constant which is equal to 96.487 C/mol.

The reversible voltage is also called open circuit voltage (OCV). The OCV assumes values between 1.25 – 0.91 V in a temperature range of 0 – 1000 °C [18].

However, because of the heat losses and thermodynamic irreversibility, in real electrolyzer the voltage needed to produce hydrogen is much higher.

The real cell voltage is given by the sum of the reversible voltage and three other overpotentials, as shown in equation (11).

$$U = U_{rev} + U_{ohm} + U_{act,anode} + U_{act,cathode} + U_{conc/diff} \qquad (11)$$
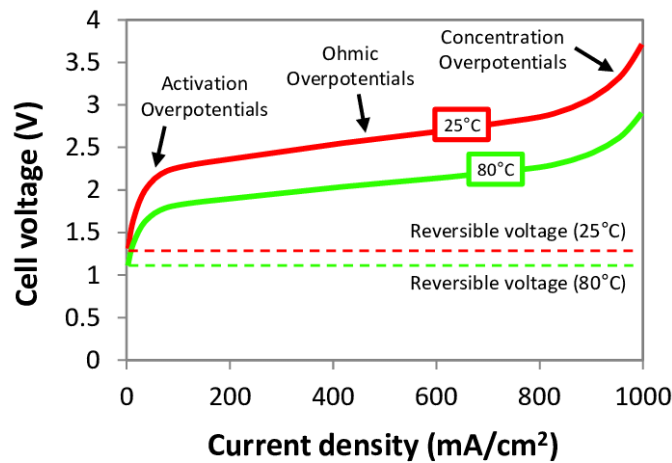
Figure 4 – Representation of a cell polarization curve [35]

These overpotentials represent three main phenomena that change the equilibrium condition of the cell.

In particular, the ohmic overvoltage (U_{ohm}) stands for the charge migration phenomenon. To overcome the resistance opposed by the membrane to the permeation of the ions and the resistance opposed by several cell elements like electrodes, interconnectors and current collectors to the electrons flow, an increment of voltage is needed.

Instead, the activation overvoltage (U_{act}) represents the charge transfer phenomenon which happens at both anode and cathode: the electrons have to overcome an energy barrier when transferring from reactants to the electrodes [17], otherwise their recombination occurs.

Finally, the concentration/diffusion overpotential ($U_{conc/diff}$) is due to the mass transport process: the molecules have to diffuse inside the electrodes and then arrive to the active point where the reaction takes place.

The overall voltage required by the cell varies with the cell temperature and with the partial pressures of the reaction's reactants and products. However, its values vary mainly depending on the current density which flows within the cell.

Furthermore, in the electrolysis process, the current density is the factor which determine the amount of hydrogen produced by the cell. Ideally, the molar flow of hydrogen produced is related to the current density by the Faraday law, expressed in equation (12).

$$\dot{n}_{H2} = \frac{i*A*N_{cell}}{z*F}$$

(12)

Where, $\dot{n}_{H2}$ is the hydrogen molar flow [mol/s];

i is the current density [A/cm^2];

N_{cell} is the number of cells in the stack;

A is the cell surface [cm^2].

Nevertheless, for real electrolysis cell, the real production of hydrogen is lower than the ideal one because of parasitic current losses in the gas pipes and cross permeation of gaseous products [17].

Therefore, the real production rate is obtained by multiplying the ideal one and the so-called Faraday efficiency.

3 Experimental activity

3.1 Objectives

The experimental activity carried out concerns an electrolyzer based on AEM technology, located in the laboratory of 'Officine Edison Torino'.

The tested electrolyzer is a small-scale commercial machine, which can produce, at rated conditions, 0.5 m3/h (25°C – 1 atm) of hydrogen at 20 bar. The system is installed within a test station where the power supply comes from the grid, but it has the possibility to be connected to a renewable source, like photovoltaic panels.

The objective of the experimental activity was to perform an assessment of the electrolyzer based on the new AEM technology. In particular, the focus was on the device performances investigation at different operating conditions, like different quantity of hydrogen produced, different operating temperature and different hydrogen production pressure conditions.

3.2 Electrolyzer description

The device consists of electrolytic stack, power supply generator, hydrogen pressure regulation, water and electrolytic solution recirculation management and cooling system.

Concerning the description of the components and materials forming the electrolyzer, no lot of information are available, since the manufacturer didn't provide any details because of the confidentiality of the data.

1   Electrolytic stack.

The stack is the main component of the electrolyzer.

It is composed of 54 cells, arranged as 2 stacks electrically in parallel, each of 27 cells in series, and each cell has a surface of 50 cm^2.

As described in chapter 2.1.1.3, the cell is made of a cathode, where the reduction reaction occurs and the hydrogen is produced, an anode, where the oxidation reaction occurs and the oxygen is delivered, and a solid membrane which is permeable to both water and hydroxyl ions.

The anodic electrode is made of Ni-Fe alloy, which is a good electronic conductor and shows a good catalytic action to oxidation reaction. Furthermore, the anode has to be porous, to allow the crossing of the water molecules towards the membrane and of the oxygen molecules that are produced by the oxidation reaction.

Regarding the cathodic electrode, its constituent material is Pt-cerium oxide. The cathode, as well, has to be porous to guarantee the passage of the produced hydrogen gas and in addition, it has to have a high electronic conductivity and catalytic activity to allow the reduction reaction.

The anion exchange membrane, instead, has to be permeable to hydroxyl ions and water, while it has to be impermeable to hydrogen and oxygen gases and it has to be an electronic insulator to avoid the short circuit of the cell. The membrane matrix is made of polyethylene and its thickness is around 50 µm.

Finally, the electrolytic solution is composed of water and 1w% of KOH.

Figure 5 represents the AEM technology on which is based the operation of each electrolytic cell of the tested device.
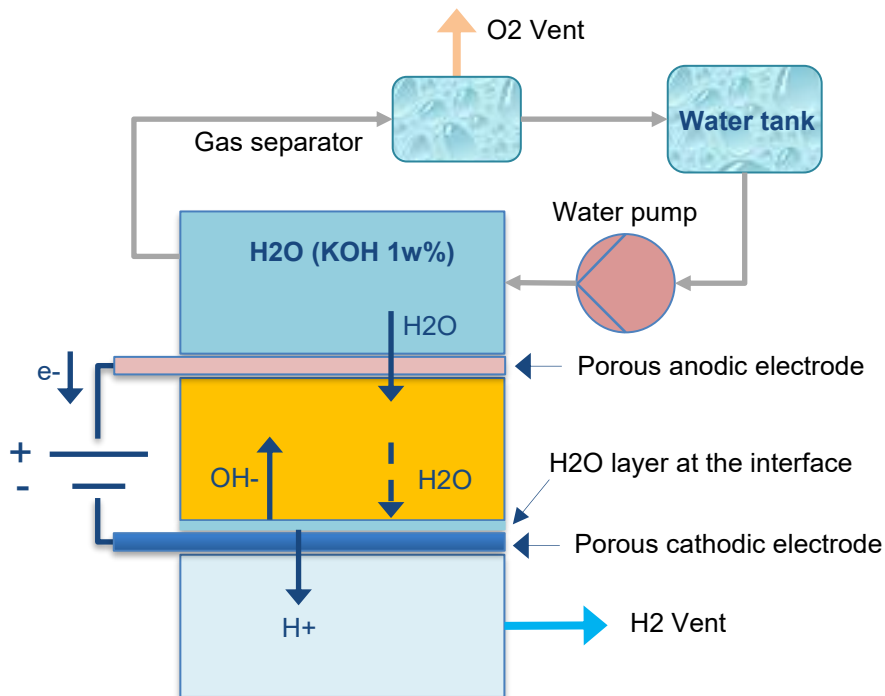
Figure 5 – schematic representation of the electrolytic cell

The electrolytic solution formed by water and KOH 1w% circulates in the anode compartment. Part of the water crosses the membrane and arrives on the cathodic surface; part exits the cell together with the produced oxygen.

The solid membrane allows both the diffusion of the hydroxyl ions from the cathode to the anode and the migration of water in the opposite direction.

As it can be noted, in the cathodic compartment, no fluid recirculation is present and it is totally saturated of only hydrogen gas, up to reach a maximum pressure of 20 bar.

Finally, the main technical stack's specifications provided by the manufacturer are reported in Table 3.

Description	Value	Unit
Production rate	0 – 0.5	Nm^3/h
Electrolysis power consumption	0 – 2.6	kW
Current density	400	mA/cm^2
Electrolysis specific energy consumption	3.9	kWh/Nm^3
Pressure output	20	bar
Working temperature	40	°C

Table 3 – Main technical specifications of AEM electrolyzer

2   Power supply generator.

The electric energy needed to the production of hydrogen is provided by the grid.

The electrolyzer is equipped with a DC current generator, controlled by a PID (proportional integral derivative) regulation system.

Depending on the hydrogen production required, by means of the Faraday law (see equation (12)), the needed current is calculated by the software managing the electrolyzer and then provided to the stack.

3   Hydrogen pressure regulation.

The tested electrolyzer is an unbalanced pressure system. The anodic compartment, indeed, is always at atmospheric pressure, while the pressure of the cathodic side can be increased up to 20 bar, by means of a back pressure valve.

The back pressure regulator is a device that maintains a defined pressure upstream of itself. When gas pressure at the valve inlet exceeds the setpoint, the valve opens to relieve the excess pressure [19]. Therefore, the valve is closed until the cathodic pressure set point is reached and then, as soon as the pressure value is exceeded, the valve opens, and the hydrogen gas can flow. When the gas pressure decreases too much, the valve closes again. Consequently, the hydrogen exits from the cathodic compartment in an irregular way.

4   Electrolytic solution recirculation management.

Figure 6 represents how the recirculation of water + KOH solution, required by the stack, is managed.

Whenever the water inside the H2O tank is below a certain level, the grid supplies water. Before filling the tank, water coming from the grid passes through a series of filters whose role is to remove minerals, ions or any impurities present in the flow.

After the filtering system and the water tank, a tank with KOH is present. The fresh water doesn't continuously fill this tank, but only when the liquid reaches a certain level, which indicates that the concentration of KOH inside the tank has exceeded 1w%.

Afterwards, the electrolytic solution passes through the cooling system and then is pumped towards the anodic compartment.

The liquid solution together with the produced oxygen gas, which exit from the stack, passes through a gas separator. Here the oxygen is vented into the atmosphere, while the remaining water goes back to the tank.
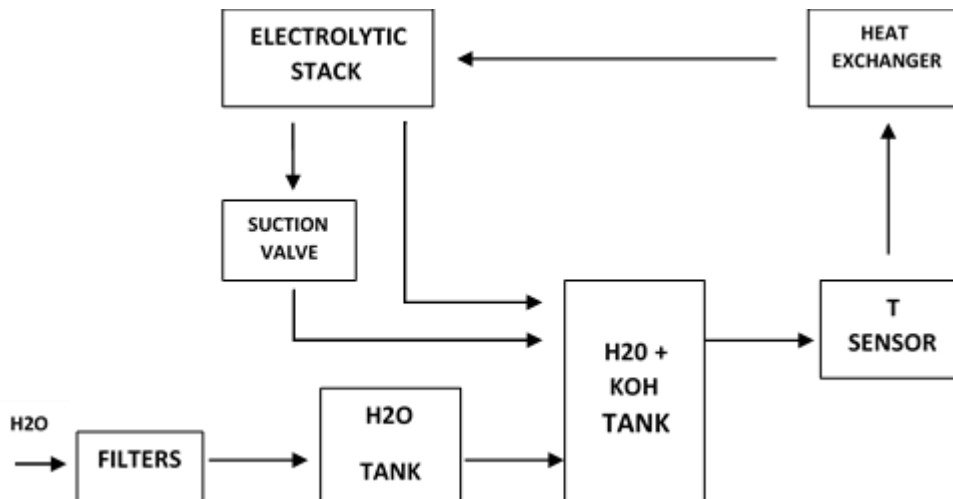
Figure 6 – Schematic representation of water and electrolytic solution management

Finally, a suction system is present. It acts every 10 minutes, and its role is to remove any moisture present along the hydrogen line, thus allowing a very high level of hydrogen purity. The water sucked returns to the tank containing H2O+KOH.

5   Cooling system.

During the electrolytic process, heat is produced. Therefore, the water that comes out of the stack has a higher temperature than the water coming in.

As it will be observed in chapter 3.5.2, high operating temperatures help the process of hydrogen production. However, it's not possible to reach too high temperatures because of the integrity of the materials forming the cells and furthermore, as reported in Table 3, the optimal working temperature is 40°C and the manufacturer selected a maximum temperature equal to 45°C. Due to all these reasons, a cooling system is required.

However, the tested electrolyzer doesn't have a thermoregulation system. The actual system, indeed, doesn't maintain the temperature at a constant value, which can be defined by the manufacturer or by the user, but it keeps it between two extreme values. In order to do that, the cooling system is composed of an

heat exchanger and of a thermometer (see Figure 6). It is not always active, but only when the measured water temperature is higher than 41°C and it stays on until the temperature is above 37°C.

It has to be noted that when the water temperature is low, since there is not a temperature control system able to increase it at rated values, the electrolyzer works in not optimal conditions.

3.3   Experimental set-up

The layout of the test station is represented in Figure 7.
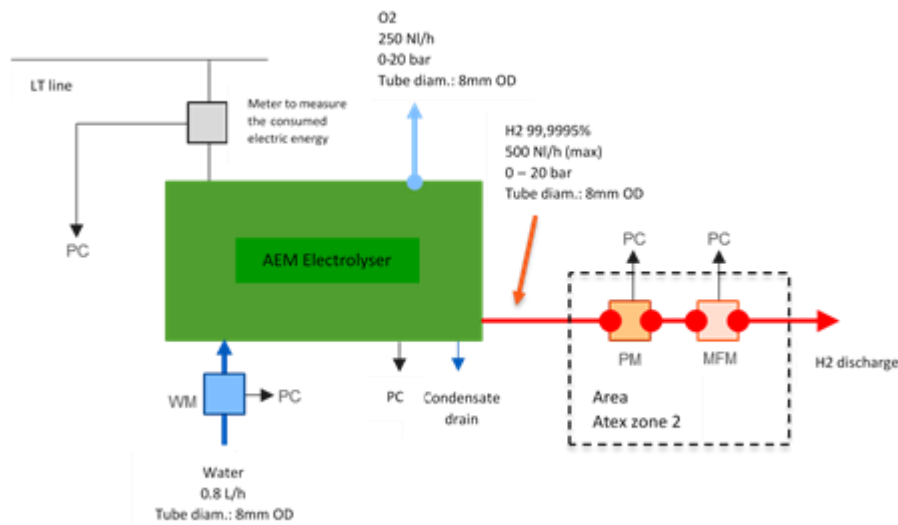
Figure 7 – Layout of the experimental set-up

The test station has been designed to measure and correlate the following variables:

- Current [A] and voltage [V] provided to the stack: these quantities are measured by means of a PLC;
- Consumed electric energy [kWh]: it is measured by means of an energy meter;
- Mass flow of consumed water [g/h]: it is measured by means of a water flow meter (WM in Figure 7);
- Hydrogen outlet pressure [bar]: it is measured at the cathodic side by means of a pressure meter integrated into the back pressure valve;
- Water temperature [°C]: it is measured by means of a thermometer which is located before the heat exchanger (see Figure 6);
- Hydrogen flux [Nl/h]: it is measured by means of a flow meter. The produced hydrogen is led inside a protected box by a small diameter pipe. Here, the mass flow meter is located (MFM in Figure 7).

In addition, Edison has developed a controller software to allow an easier handling of the tests and of the data acquisition.

In this way, two variables are editable: the hydrogen volumetric flow and the hydrogen outlet pressure. The former can be changed from 1 to 500 L/h, while the latter from 1 to 20 bar. After setting these parameters, the current needed to produce the required hydrogen will be provided to the stack and the set-point of the back pressure valve will be regulated, respectively.

Furthermore, the software allows also to read the measures given by the sensors listed before.

A picture of the test bench is reported below.

Figure 8 – Picture of the test bench

3.4   Measurements' uncertainty

Following, the uncertainty related to the variables' measures due to instrumental errors are listed.

- Voltage and current measurements.

The values of the electrical quantities are measured by a transducer (PLC). It is characterized by a resolution of 16 bit and it converts signals in the range of 0-10 V (0-10 A).
Therefore, each measurement is characterized by a quantization error of:

$$Q = \frac{E_{ref}}{2^N - 1} = \frac{10000}{2^{16} - 1} = 0.15 \, mV/bit$$

Thus, the errors affecting the voltage and current values are respectively ±0.0002 V and ±0.0002 A.
The measures are repeated 100 times in 10 seconds and then a mean value is calculated. However, the error of such value remains the same.

- Hydrogen pressure measurement.

The sensor is characterized by a linearity lower than ± 0.1% FSO. Therefore, the error affecting the pressure measurements is $\pm \frac{0.1*20}{100} = \pm 0.02 \, bar$.
The measures are repeated 100 times in 10 seconds and then a mean value is calculated. However, the error of such value remains the same.

- Hydrogen flow measurement.

The flow meter is characterized by a sensibility of 0.4% of the reading value.

Below, instead, the errors of the computed parameters, due to measuring devices uncertainties, are reported.

- Power required by the stack.

Since the power is calculated as a product between voltage and current, its uncertainty is given by:

$$\delta P = I * \delta V + V * \delta I \qquad\qquad (13)$$

Depending on the production, since both the voltage and the current values vary, the uncertainty changes, but it is always very low and around ± 0.01 W.

In particular:

Set point production	Power uncertainty
500 Nl/h	± 0.018 W
400 Nl/h	± 0.017 W
300 Nl/h	± 0.015 W
200 Nl/h	± 0.013 W
100 Nl/h	± 0.011 W

Table 4 – Power uncertainty

- Stack efficiency.

Since the efficiency of the stack is calculated as a ratio between the LHV of hydrogen and the stack power times the hydrogen mass flow, its uncertainty is given by:

$$\delta\eta = \frac{LHV}{Power_{stack}}\left(\delta\dot{m}_{H2} - \frac{\delta Power_{stack}}{Power_{stack}}\dot{m}_{H2}\right) \tag{14}$$

It depends on the amount of hydrogen produced per hour. However, as Table 5 shows, it varies only of cents of percentage and its value is always around ±0.2%.

Set point production	Stack efficiency uncertainty
500 Nl/h	±0,24%
400 Nl/h	±0,23%
300 Nl/h	±0,22%
200 Nl/h	±0,22%
100 Nl/h	±0,17%

Table 5 – Stack efficiency uncertainty

As it can be noted, all measuring instruments are very precise. The main sources of uncertainty on the measures, indeed, are not the measuring devices but other factors which depend on the electrolyzer's design. As reported in the following pages, these factors are the not constant operating temperature and cathodic

pressure, and the variable produced hydrogen flow rate. They contribute to having a cloud of measures for the same operating conditions and thus, the results of the experimental tests are characterized by high deviation.

Therefore, summarising, the errors due to the measuring system are negligible and the ones shown later are only due to the measurements' deviation.

It should be noted that all results that will be presented in this work are integral averages of all data measured in each test carried out.

In addition, each result is provided with its uncertainty. The latter is calculated by multiplying the standard deviation by the z-value equal to 1.96, in order to have a result characterized by a confidence level of 95%.

3.5   Experimental tests and results

Different tests have been conducted to evaluate the performances of the electrolyzer.

In particular, in the first place, the goal of the tests was to observe the behaviour of the device with the variation of the 3 main parameters: operating temperature, hydrogen production level and hydrogen outlet pressure.

Secondly, the data have been analysed to identify the optimal working point.

Every test has been carried out for one working day, from around 9 a.m. to around 5 p.m. In addition, the first minutes of each test have not been considered during the data analysis, in order to eliminate the data referring to not still stable working conditions.

3.5.1   Real hydrogen production

The device has the functionality of allowing the user to set the hydrogen volumetric flow to produce. However, it has been observed that there is a mismatch between the setpoint production level and what is measured by the hydrogen flow meter. In fact, the technical specifications reported a maximum hydrogen production capacity for the tested electrolyzer around 0.5 m^3/h, but actually, its maximum production is around 0.4 m^3/h.

Figure 9 reports the comparison between the setpoint production and the measured production for different hydrogen pressures, where all values have been referred to the normal conditions: temperature equal to 273 K and pressure equal to 1 atm.

As it can be observed, the values of the real productions change with the hydrogen outlet pressures.

In general, at each setpoint production the measured gas flux is higher at 1 bar than at 20 and 10 bar. For instance, when the setpoint is equal to 92.3 Nl/h, the real production at 1 bar is 55 Nl/h, while at 20 bar is 43 Nl/h and at 10 bar is only 28 Nl/h.

Therefore, it can be stated that the electrolyzer is capable of producing higher amount of hydrogen when the cathodic pressure is the atmospheric one.
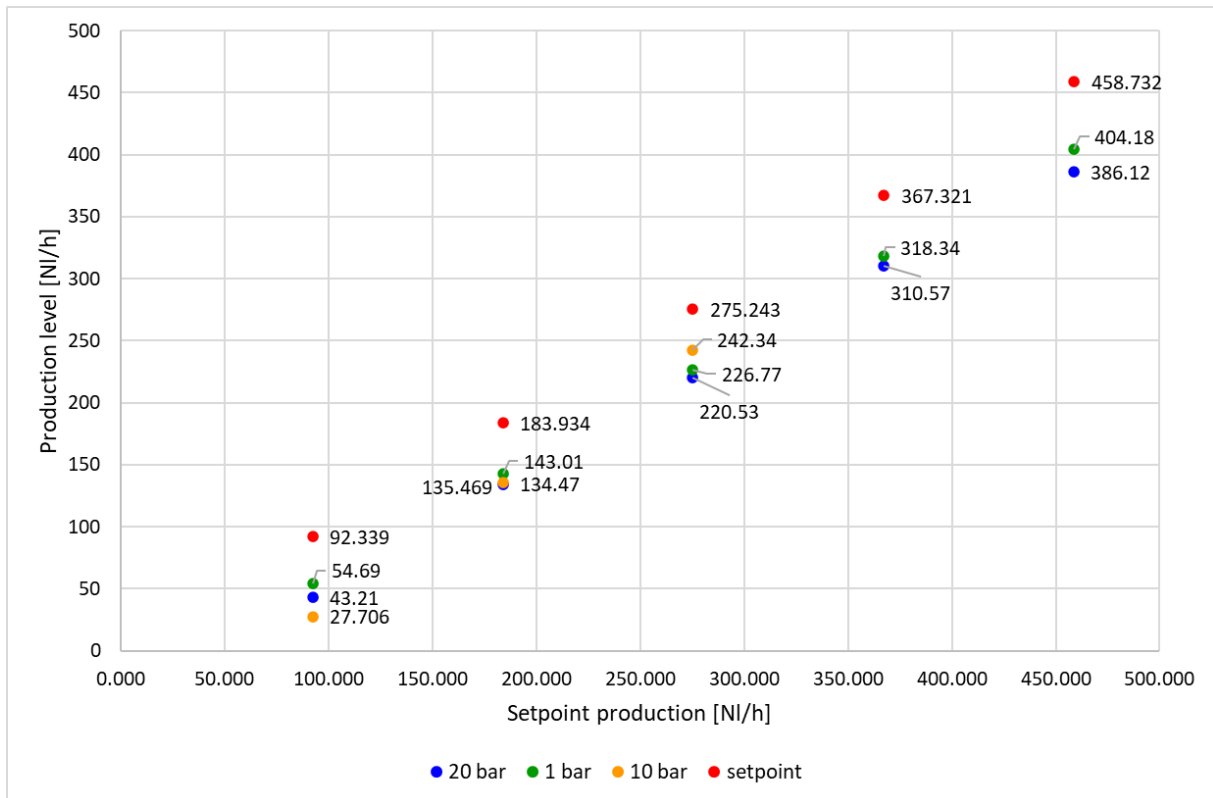
Figure 9 – Comparison of setpoint production levels and measured production levels

The production levels reported in Figure 9 are integral mean values of all measures done during each test.

It has to be noted, indeed, that the hydrogen doesn't come out of the electrolyzer at a constant flow rate, even though the setpoint production is kept constant. The hydrogen flow meter sometimes measures very different values, depending on the set PID parameters effectiveness.

However, at some working conditions the production is more stable than in other. Figure 10 represents, at each cathodic setpoint pressure, the mean hydrogen production level and its standard deviation when the setpoint production has been set to 300 L/h.
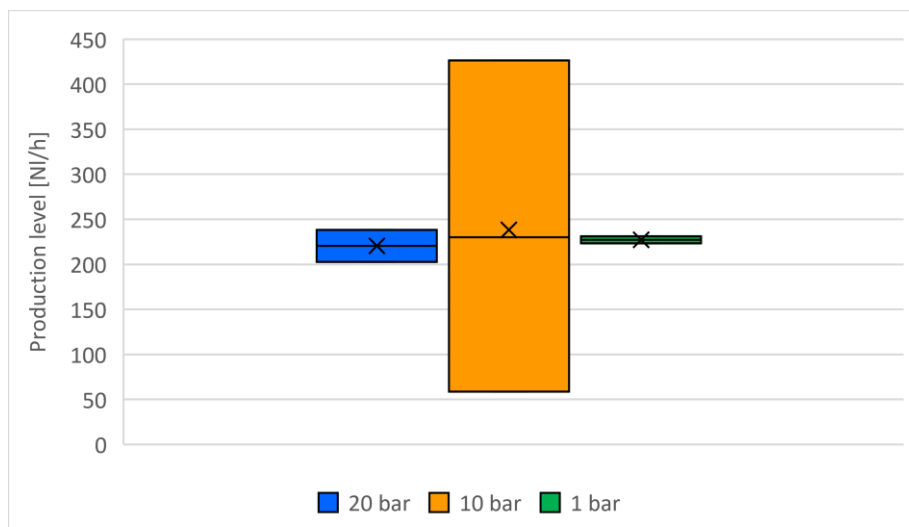
Figure 10 - Representation of the mean production level and its standard deviation for different hydrogen outlet pressures, when the setpoint production is equal to 300 l/h

It can be observed that when the pressure is equal to 10 bar, the standard deviation is very high. It means that the production value fluctuates a lot. Instead, when the pressure is 20 bar or 1 bar, the electrolyzer is able to produce the gas at more constant flow rate.

Only the case of the setpoint production equal to 300 l/h has been reported, but the same results were observed for all other setpoints.

This observation leads to assert that the back pressure valve doesn't work properly when the cathodic pressure is set to 10 bar and therefore, the measured data are affected by too high uncertainty. That's why only the data referring to a hydrogen pressure equal to 1 and 20 bar have been analysed and in the following sections, only these results are reported.

In addition, it should be noted that from this point forward, the hydrogen production values that will be reported are the measured ones.

3.5.2   Influence of the operating temperature on the electrolyzer performances

To observe the response of the electrolyzer at the variation of the working temperature, the production level and the hydrogen outlet pressure have been maintained constant.

- Measured temperature.

As highlighted in chapter 3.3, the cell operating temperature is not an editable parameter since there is not a thermoregulation system.

Furthermore, the measured temperature doesn't correspond to the cell temperature. As shown in Figure 6, indeed, the thermometer provided by the manufacturer is located outside of the stack.

The measured temperature is not representative of the temperature of the water coming out of the stack, because it's the temperature of that water mixed with the fresh one. It doesn't even correspond to the temperature of the water entering the stack, because it is measured before passing through the heat exchanger.

Therefore, two thermocouples have been installed close to the stack, in particular on the pipes containing the incoming water and the outgoing water.

Then, the measures of the two new sensors and of the system thermometer have been compared, as shown in Figure 11.
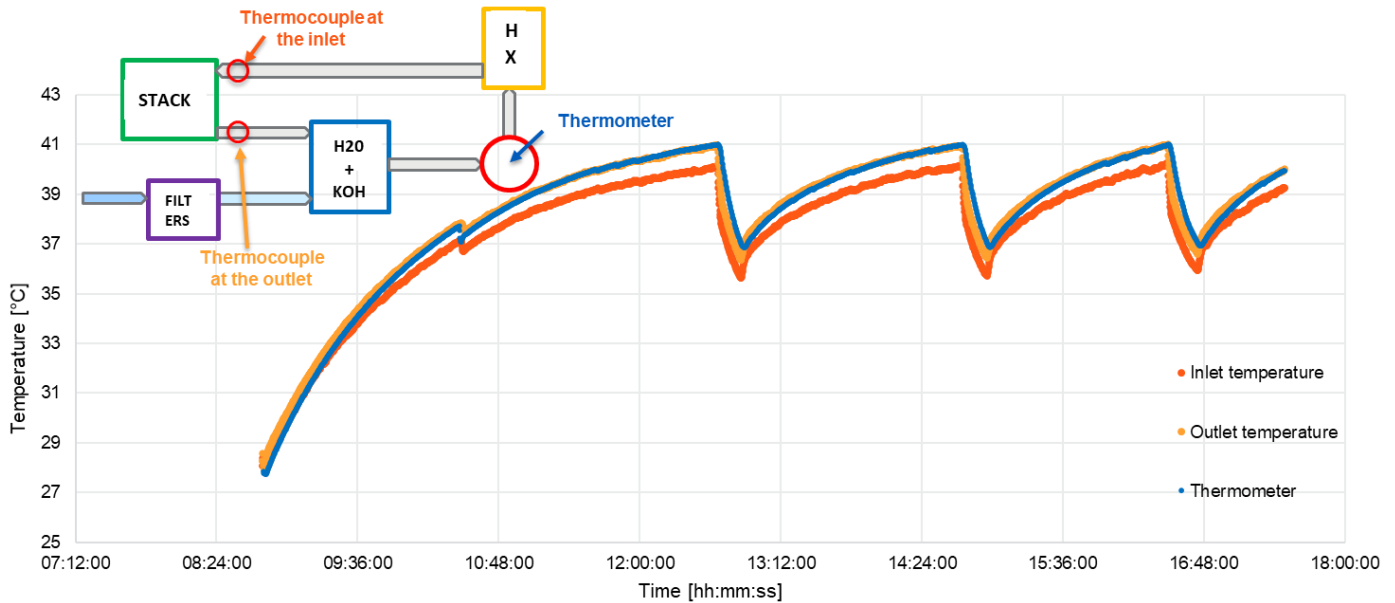
Figure 11 - Comparison of the temperature's measures

As it can be seen, the measures differ by a few degrees, but they all follow the same trend.

As expected, the temperature of the water coming into the stack is lower than the one of the water coming out. It is also lower than the temperature measured by the thermometer, due to the presence of the cooler right behind.

From this point forward, the measured temperature will be treated as the cell operating temperature.

As shown, it's an approximation because the two temperatures are not exactly equal, but it's deemed more significant the temperature's variation, which is the same for all the used sensors.

- Influence of the external conditions on the operating temperature.

Due to the lack of a temperature control system, the working temperature is affected by the ambient temperature, as visible in Figure 12.

These data are referring to a 300-hours test period, having been set the production level at 100 l/h and a cathodic pressure equal to 3 bar.

It can be noted that the temperature oscillates on daily basis. In particular, during night, when the ambient temperature is colder, the water temperature decreases.
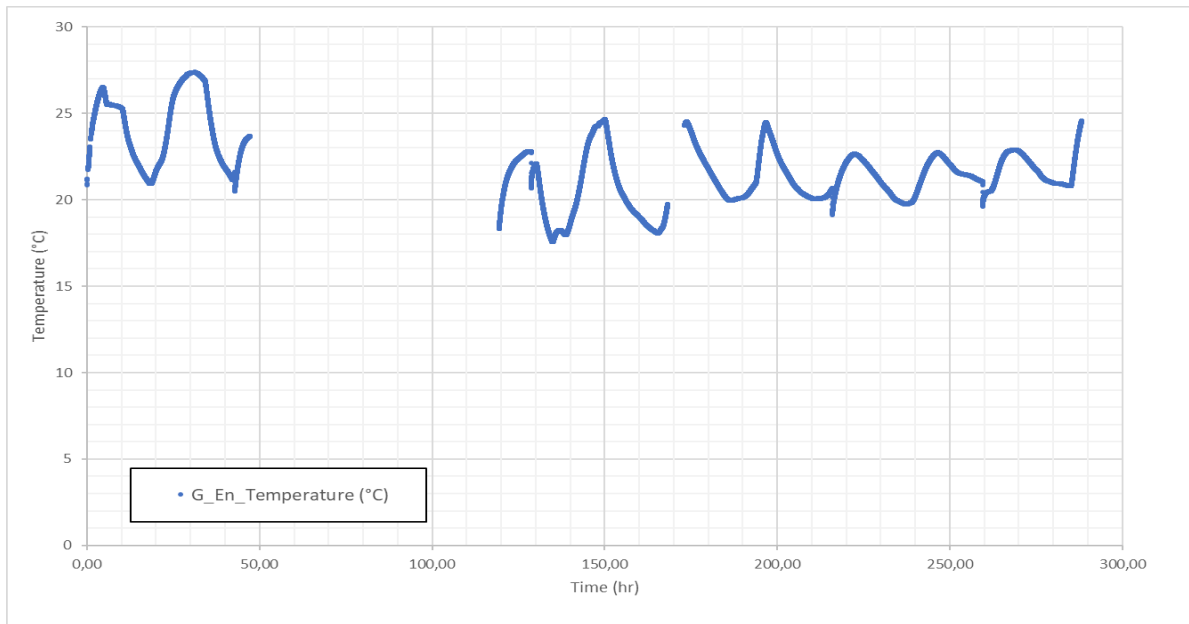
- Influence of the operating temperature on the performance of the electrolyzer.

For each test carried out, the hydrogen pressure and the production level have been kept constant and the variation of the main stack parameters, voltage and current, with temperature have been observed.

For each production and pressure set point, always the same results have been obtained: the voltage changes with temperature, while the current stays constant. (Figure 14)

The current doesn't vary because it is influenced only by the hydrogen production. The electric generator, indeed, provides current to the stack on the basis of the Faraday law and therefore depending on the hydrogen production that has been set.

Regarding instead the voltage, as visible in Figure 13, whenever the temperature increases, this parameter decreases following a linear relationship.
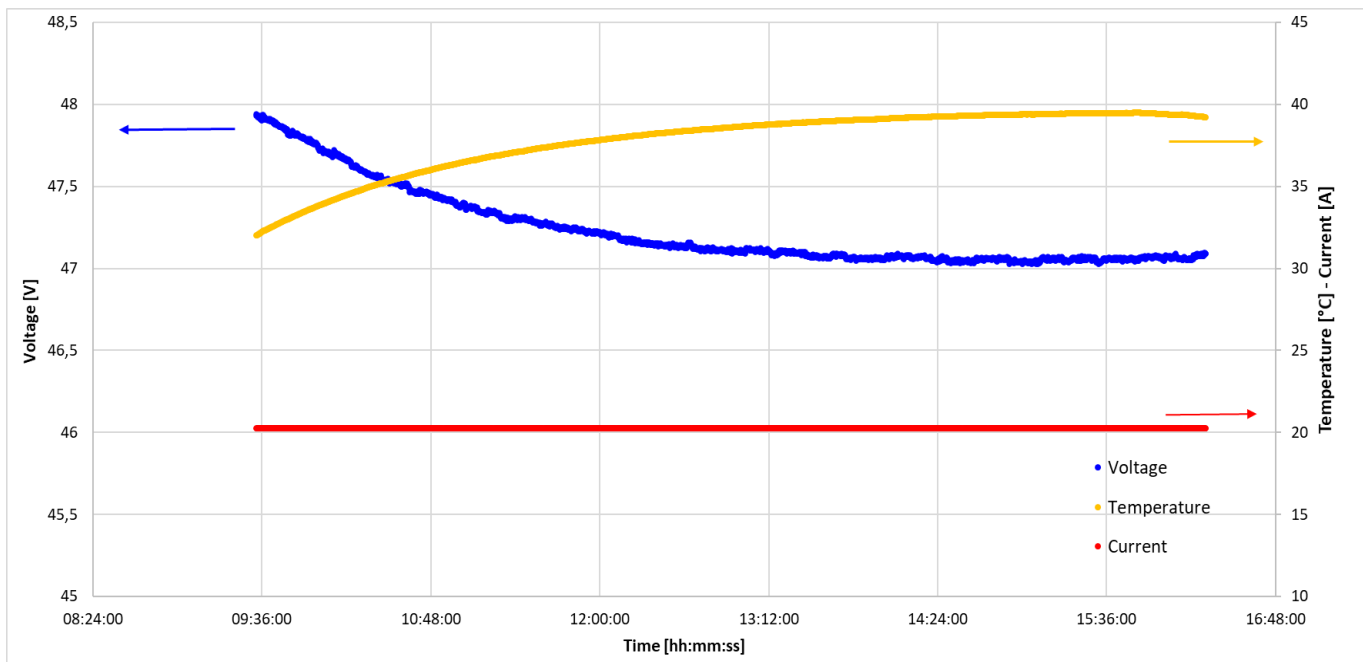
Figure 14 - Voltage, Temperature and Current VS Time – H2 production of 250 l/h and H2 pressure equal to 10 bar

$$y = -0{,}123x + 51{,}879$$
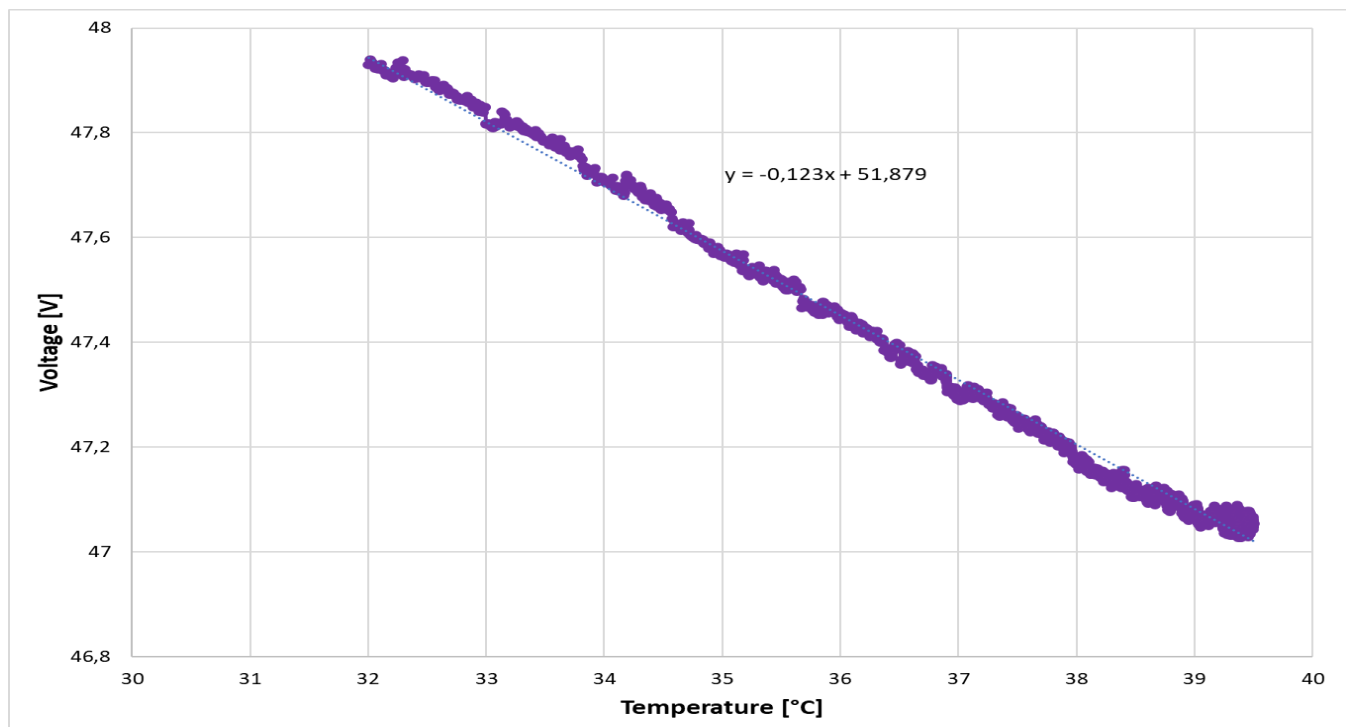
Figure 13-Voltage VS Temperature - H2 production of 250 Nl/h and H2 pressure equal to 10 bar

In the case reported in Figure 13, in a temperature range of around 7°C, the voltage varies of around 0.9 V. Furthermore, it has been observed that, depending on the gas production setpoint and cathodic pressure setpoint, the voltage variation per degree of temperature changes without showing a specific trend. However, the variation is never higher than 0.2 V/°C and, in particular, it stays in a range of 0.08 – 0.2 V/°C.

Starting from the voltage and current data, the stack efficiency has been computed using equation (10).

$$\eta = \frac{\dot{Q}_{H2} * LHV}{V * I}$$

(15)

Where, $\dot{Q}_{H2}$ [Nl/h] is the hydrogen volumetric flow measured by the flow meter;

LHV is the hydrogen lower heating value, which is equal to 3 Wh/NL (in normal conditions, T=0°C and p=1 atm);

V is the voltage across the stack;

I is the current flowing into the stack.

Consequently, decreasing the voltage with temperature, staying constant the current and not varying the hydrogen production, the efficiency should increase with the operating temperature.

However, this is not visible by looking at the measured data. In fact, as observed in paragraph 3.5.1, the real hydrogen production is not constant, but it fluctuates a lot. Therefore, the effect of temperature on the stack efficiency is not visible: the influence of measured hydrogen flow's variation on the efficiency values is greater than the influence of the voltage's variation with temperature.

3.5.3   Influence of the hydrogen production level on the electrolyzer performances

To evaluate how the hydrogen production level affects the performance of the electrolyzer, during each test the cathodic pressure has been kept fixed.

As expected, the variation of the production setpoint causes a variation of both current provided to the stack and voltage across it.

Figure 16 reports the relationship between the cell current density and the hydrogen flowrate. The cell current density has been computed as:

$$i = \frac{I/2}{A_{cell}}$$

(16)

Being, I/2 the current flowing through each cell (the stack is composed of a parallel of cells);

A_{cell} the surface of each cell, which is equal to 50 cm^2.

Whenever the current density increases, the hydrogen production increases as well.

In the case of an ideal electrolyzer, the relationship between the two variables would be linear and it would correspond to the Faraday law.

However, it can be noticed that, in the case of the tested electrolyzer, the relationship between the two variables is not exactly linear and in addition, the measured production values are lower than the ideal ones. In fact, being the electrolyzer a real device, its production is affected also by other factors, as will be described in chapter 3.6.1.
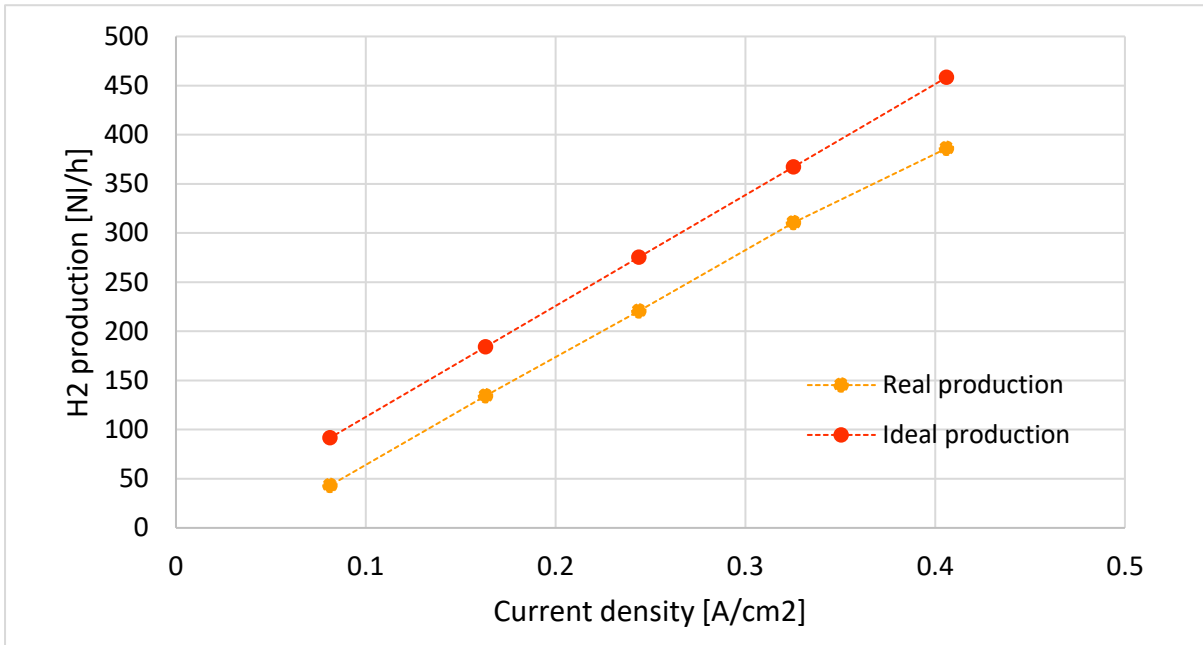
Figure 16 – Ideal and real hydrogen production VS current density

The stack voltage, as well, increases with the hydrogen production level, as can be seen in Figure 15, which is referred to the case of hydrogen outlet pressure equal to 20 bar.
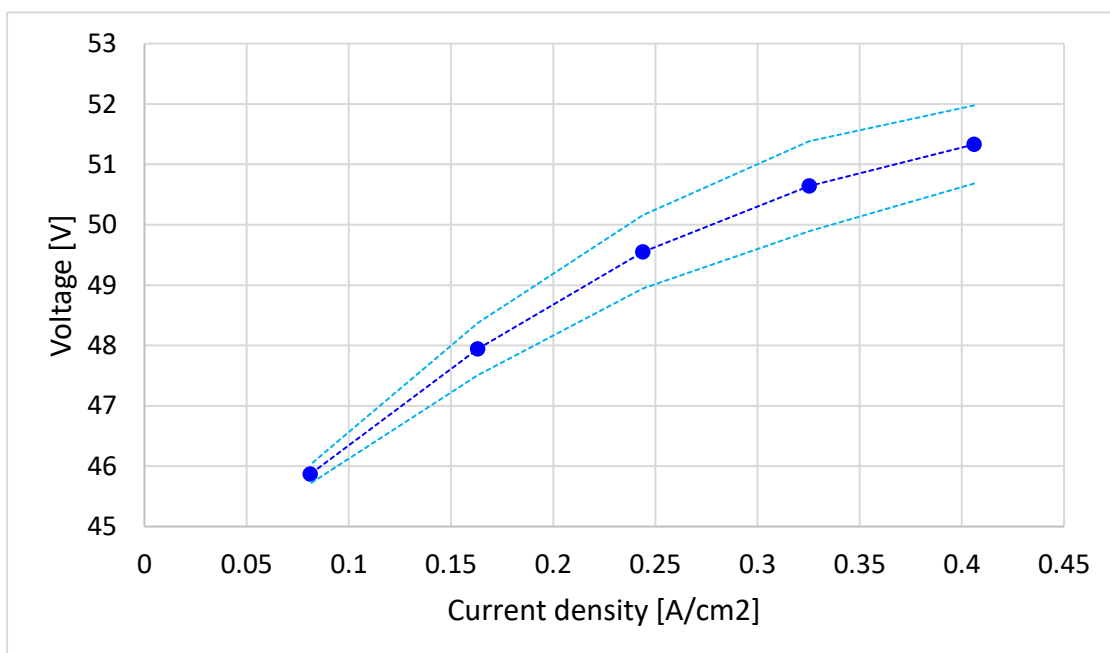
Figure 15 – Representation of the polarization curve and the uncertainties related to the voltage values (confidence level = 95%). (Case of H2 pressure = 20 bar)

The voltage trend with respect to the current density follows the thermodynamic laws reported in chapter 2.1.3.

Considering the stack efficiency, its increment with the production level has been observed. It varies from around 35% when the electrolyzer produces 43 Nl/h to around 56% when the production is 386 Nl/h. However, these values are affected by high uncertainty, as visible in Figure 17 where the variation of the efficiency and its uncertainty, with respect to the produced hydrogen flowrate, are reported.
There are two parameters which cause this high uncertainty. One is the variation of voltage because of not constant temperature and the other one, which is the most significative, is the not constant production. At higher current densities, where the production is more stable, indeed, the uncertainty is lower. In particular, it decreases with the rise of production, passing from 39% to 12.8%.
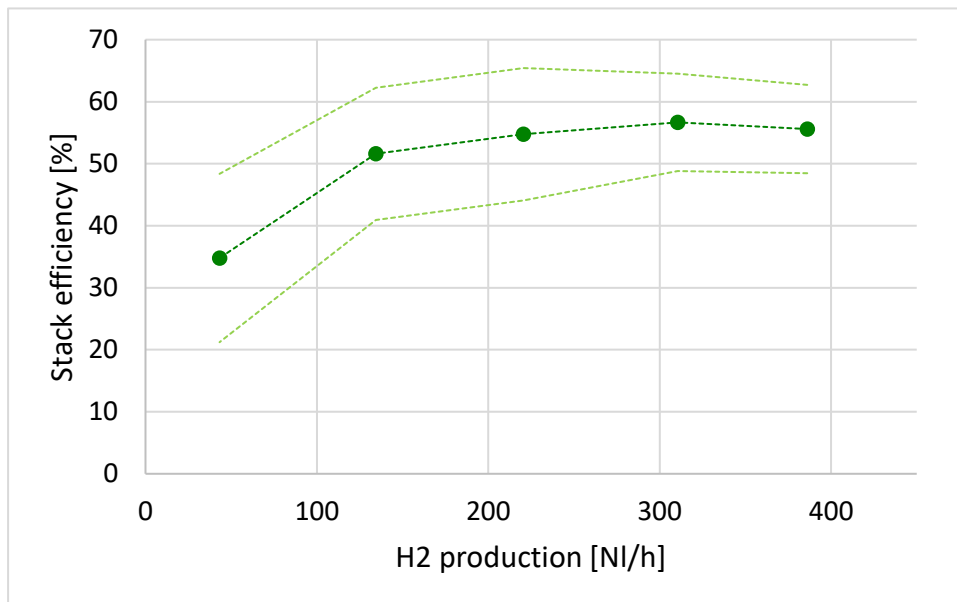
Figure 17 – Stack efficiency and its uncertainty VS hydrogen production (Case of hydrogen pressure= 20 bar)

3.5.4   Influence of the hydrogen outlet pressure on the electrolyzer performances

To analyse the influence of the hydrogen outlet pressure over the performances of the electrolyzer, many tests have been conducted. During each one, a different pressure and a different production level were set. Finally, all the data have been analysed and the results compared.

Firstly, it has been noticed that, starting from the same current provided to the stack, the electrolyzer produces an higher quantity of hydrogen at 1 bar rather than at 20 bar. The reasons why these results have been obtained will be explained in more details later on, in chapter 3.6.1.

As expected, as the operating temperature, also the cathodic pressure doesn't affect the current flowing into the stack. Instead, the pressure influences the voltage values.

However, there are some limitations due to the system configuration which do not allow to see in a clear way the voltage response:

- The operating temperature varies continuously during each test of around 5°C;
- The pressure level is not stable. Even if only slightly (tenths of bar), it varies continuously during each test. Furthermore every 10 minutes, the pressure level is disturbed because of the presence of the suction system which remove any moisture on the hydrogen line;
- The setpoint pressure doesn't correspond to the real measured pressure. In addition, the reached pressure is not always exactly the same for each test. In particular when it is set 0 relative bar, depending on the test, the actual one is in between 0.6 and 2.12; when it is set to 20 bar, the pressure varies between 17,6 and 19.2 bar.

To solve the problem of the variable temperature, it has been decided to "normalize" all the voltage values, obtained during tests at different operating conditions (pressure and production level), at one unique level of temperature. Since, as seen in Figure 13, the voltage varies in a linear way with the temperature, for each test the relationship between these 2 variables has been obtained by using the least square method. Then, it has been observed which operating temperature was reached during all the tests, in order to try to minimize the error of this approximation. Finally, the voltage values related to that temperature for all the tests have been computed.

The following figure shows the polarization curves in the case of hydrogen pressure equal to 1 bar and 20 bar, when the voltage values are related to an operating temperature of 36°C.
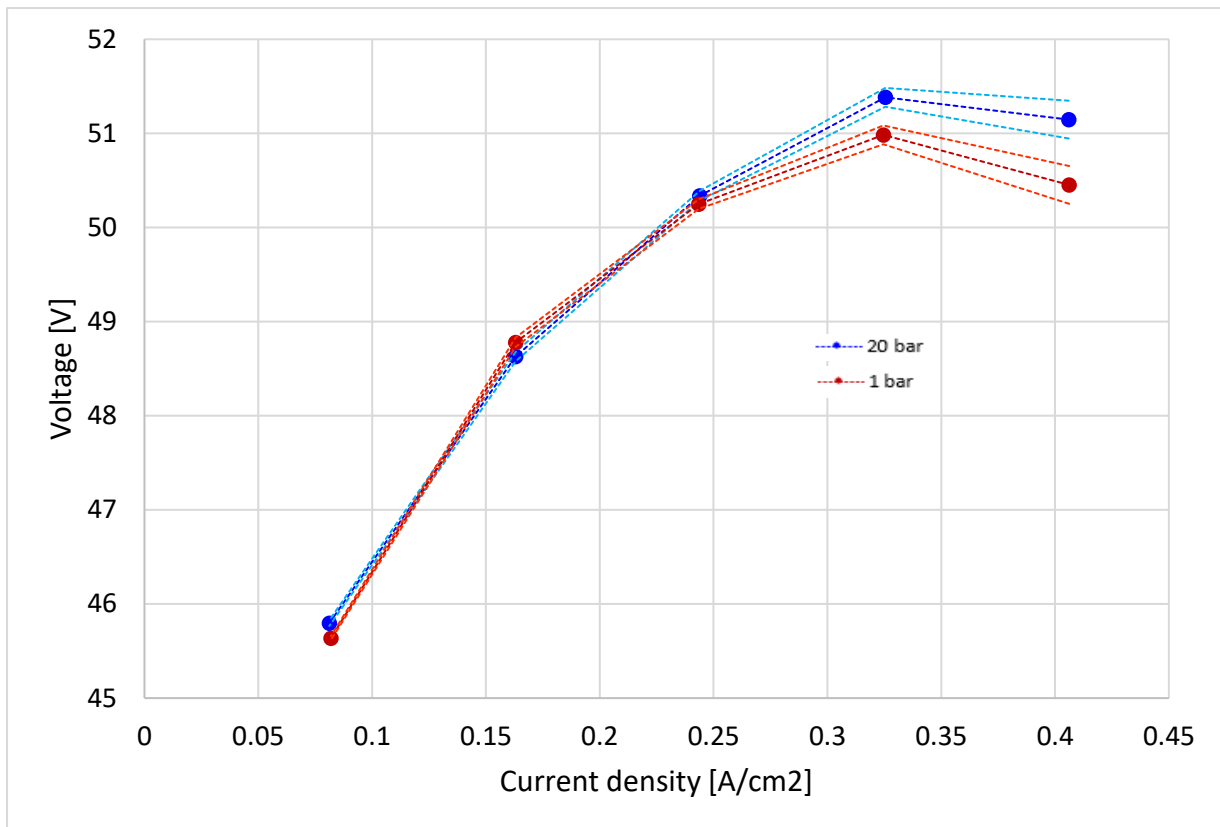
Figure 18 – Polarization curves for 2 different values of hydrogen pressure at an operating temperature of 36°C

It's observable, especially at higher current densities, that the voltage required by the stack is lower when there is no pressure difference between anode and cathode. In particular, when the current density is equal to 0.32 A/cm2 the difference between the voltage required at 20 bar and 1 bar is 0.4 V, while, when the current density is 0.4 A/cm2, the difference is 0.7 V. These results indicate a very little variation of voltage per bar, in the order of hundredths of volts per bar.

As regards current densities lower than 0.25 A/cm2, the influence of the cathodic pressure on voltage is even less significant. At 0.16 A/cm2, the graph shows a lower voltage in the case of 20 bar, which is an opposite result compared to the previous ones.

 Looking at the stack efficiency, in accordance with the previous results, the following trend should be visible: at high current densities the efficiency should be greater when the hydrogen is produced at 1 bar than when it is produced at 20 bar.

Rather, the measured data are shown in Figure 19, with their uncertainty. Considering the mean values, as expected, the stack efficiency is higher when the hydrogen is produced at atmospheric pressure, for every current density. However, this conclusion cannot be affirmed, just by looking at these results, because of the high uncertainty of the data. In fact, especially when the cathodic pressure is set to 20 bar, because of the

big hydrogen production variation, the stack efficiency varies a lot. Its values vary from 13% at 0.4 A/cm2 to 39% at 0.08 A/cm2.

However, when the electrolyzer produces hydrogen at atmospheric pressure, the stack efficiency varies from a minimum of 44% to a maximum of 58.8% when the current density passes from 0.08 A/cm2 to 0.4 A/cm2, respectively.

Instead, when the gas pressure is set to 20 bar, the stack efficiency varies from a minimum of 35% at a current density of 0.08 A/cm2 to a maximum of 57% at a current density of 0.32 A/cm2.
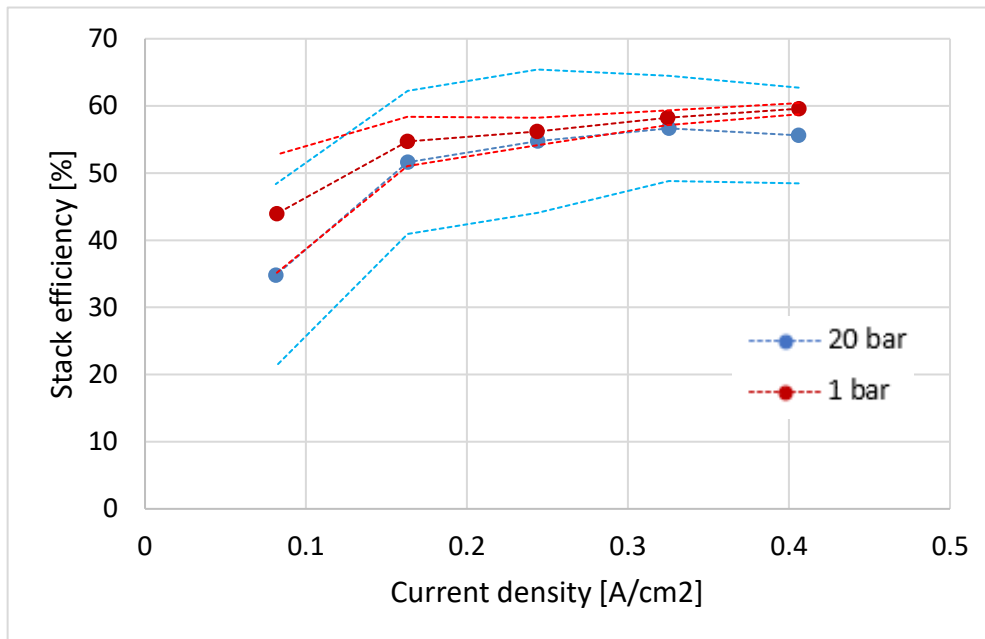
Figure 19 – Stack efficiency VS Current density for 2 values of H2 pressure

3.6 Results' discussion and theoretical explanation

3.6.1 Hydrogen production – Faraday efficiency

As already observed in chapter 3.5.1, there is a mismatch between the hydrogen production setpoint and the measured production. Furthermore, this difference varies depending on the production level and on the hydrogen outlet pressure.

To better identify the working conditions which allow a production as close as possible to the setpoint value, a new parameter has been computed, called Faraday efficiency. It is defined as the ratio between the real hydrogen production rate and the theoretical one, which is obtained by knowing the current provided to the cells. Equation 17 reports the formula used.

$$\eta_{Faraday} = \frac{\dot{Q}_{measured}[0°C, 1\ bar]}{\dot{Q}_{theoretical}[0°C, 1\ bar]} \tag{17}$$

Where, $\dot{Q}_{measured}$ is the average of the volumetric flow rates measured during the test;

$\dot{Q}_{theoretical}$ is the average of the theoretical productions computed at each instant of the test, based on the current flowing within the stack.

Keeping constant the cathodic pressure and the production level setpoints, the Faraday efficiency assumes many and different values because of the not constant hydrogen production. This is due, as already said, to the pressurization system of the cathodic compartment which opens and closes continuously the gas escape valve. Furthermore, every 10 minutes the pressure value drops down and, since the gas isn't delivered, the flowmeter measures a production equal to zero.

Therefore, to get clearer results, all the Faraday efficiency's values corresponding to nil production have been deleted during the data analysis. Figure 20 shows the Faraday efficiency as a function of the cell current density, for 2 different values of hydrogen outlet pressure.

As the current density increases, the Faraday efficiency increases as well. In particular, the efficiency decreases significantly with decreasing i, when i<0.3 A/cm2. For higher current densities, its values are quite stable. This observation finds confirmation in some scientific studies. [20]

It is possible to notice that, in general, as already observed, under the same operating conditions the electrolyzer is able to produce higher quantities of hydrogen at atmospheric pressure than at 20 bar.

When the hydrogen is produced at atmospheric conditions, the Faraday efficiency passes from 60.5% at 0.08 A/cm2 to 88.2% at 0.4 A/cm2, which corresponds to the maximum value. Instead, when the hydrogen is produced at 20 bar, it passes from 55.6% at 0.08 A/cm2 to 87.5% at 0.4 A/cm2.
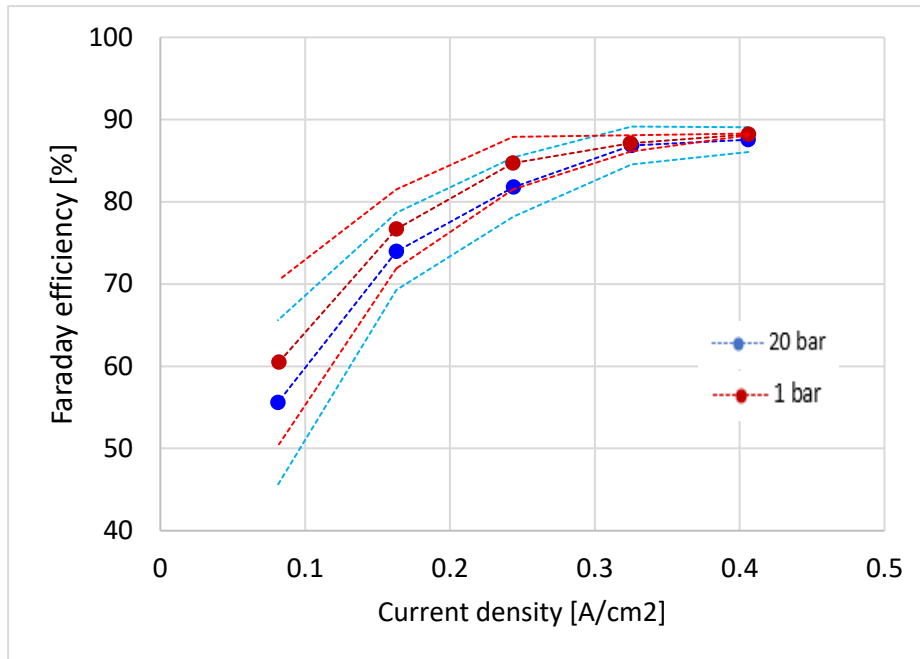
Figure 20- Representation of the Faraday efficiency with its uncertainty VS Current density, for 2 levels of hydrogen pressure

Differently from the obtained results, experimental studies, found in the literature, show much higher values of Faraday efficiencies. They reach 98 – 99% when the hydrogen rated flowrate is produced at a pressure of 1 bar ([20] - [21]). It should be noted that these experiments were performed on a laboratory scale and thus, it's reasonable that the Faraday efficiency of a commercial device is lower.

However, there are several reasons that cause this low Faraday efficiency.

In the first place, the back pressure valve operation. Since the cathodic pressure varies a lot, the valve opening doesn't remain fix and it doesn't allow the exit of all the hydrogen produced.

Secondly, the not constant operating temperature. In fact, the difference between actual and theoretical production increases with rising temperature [17].

As for the difference between the production at 20 bar and at 1 bar, according to the theory, several explanations can be found.

Driven by the pressure difference between the two electrodes, part of the produced hydrogen at the cathode tends to permeate to the anode through the membrane and the permeation flux increases with increasing the cathodic pressure [20].

There are also other reasons for this observation, but still unclear. However, previous studies demonstrated that a cause of production loss was the parasitic current losses in the gas pipes [17].

3.6.2 Temperature and pressure influence

Results in chapter 3.5.2 showed a decrement of voltage with the operating temperature increment. This in turn results in consumption of less power for a particular production rate and therefore to a better performance of the electrolyzer.

This observation is confirmed by the theory. At higher temperature, the kinetics of the charge transfer reaction improves at the electrode-membrane interface. In addition, the conductivity of the membrane increases with the increase in temperature, and this results in lower ohmic overvoltage at higher temperatures [22].

Furthermore, it has been noted that, as the hydrogen production level increases, the cell temperature increases as well. In fact, due to the anion exchange membrane resistance, more heat is delivered by joule effect as the hydroxyl ions permeation increases.

In chapter 3.5.4 it has been observed how the hydrogen outlet pressure affect the performances of the electrolyzer.

The cathodic pressure has a double effect on the cell polarization and thus on the power requested by the stack:

-   negative effect: an increase in cell pressure increases the partial pressures of the species which in turn increase the open circuit voltage calculated using Nernst equation [22];
-   positive effect: the pressure increase decreases the anode activation, cathode activation, and ohmic overvoltages. This is due to the reduction of the volume of hydrogen bubbles occupying the electrolyte and covering the active area of the electrode surface and thus to the of the electrolyte and electrode resistances, because of decrement of hydrogen bubbles sizes with increasing pressure [23].

As Figure 18 showed, at low and high loads, the Nernst effect is the predominant one: increasing the cathodic pressure, the required voltage increases. Furthermore, according to literature and confirmed by the experimental results, the pressure effect is more prominent at high current densities [22].

Instead, at intermediate loads, the pressure positive effect prevails.

In addition, if it were possible to fix the cell temperature, the cathodic pressure effect would be more evident at lower temperatures [22]. In fact, this observation is visible by comparing the polarization curves obtained by referring all the voltage values to 36°C and then to 41°C through the least square method (Figure 21).

It is possible to notice that the biggest difference, between the curve referring to a pressure of 20 bar and the curve referring to 1 bar, is obtained at the lowest operating temperature.
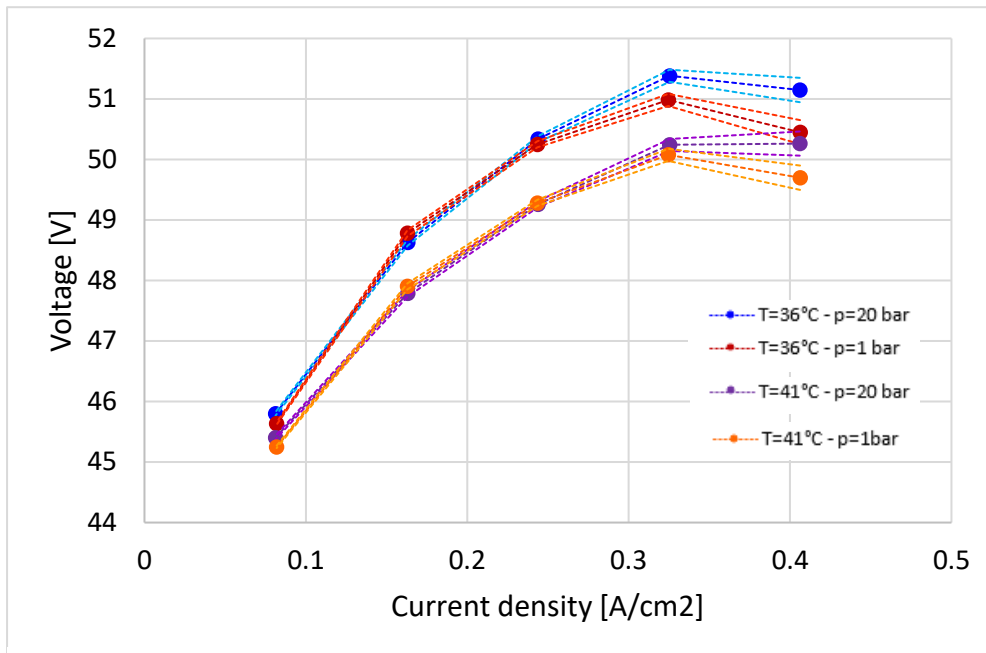
Figure 21 – Polarizations curves for different operating temperatures and H2 pressures

Furthermore, by analysing the previous graph, it is possible to conclude that the operating temperature has a greater effect on the electrolyzer's performance than the gas outlet pressure.

By performing the ANOVA analysis, it has been confirmed that the voltage's variation because of cell temperature's and hydrogen pressure's variation is a real phenomenon and it is not the result of the measures' uncertainty. This statistical analysis has been performed for 3 different values of current densities, by comparing the voltage's values measured at 2 levels of operating temperature (37°C – 41°C) and 2 levels of cathodic pressures (1 bar – 20 bar).

The results reported in Table 6 show that, at current densities higher than 0.24 A/cm2, both the operating temperature and hydrogen outlet pressure have a statistically significant effect of the performance of the electrolyzer (p-value <0.05, confidence level > 95%). While, regarding current densities equal and lower than 0.24 A/cm2, only the temperature effect is statistically significant. It has been already noted, indeed, that at low production levels the pressure affects in a very little way the voltage's values.

However, the pressure has again a statistically significant influence on the stack voltage when the current density is equal to 0.08 A/cm2.

Furthermore, for all the current densities, the temperature has a p-value lower than the pressure. It means that the aforementioned statement, about the greater effect of the operating temperature than the cathodic pressure over the electrolyzer performance, is confirmed.

		p-value
i=0.4 A/cm2	Temperature effect	0.001
	Pressure effect	0.0016
i=0.32 A/cm2	Temperature effect	0.0004
	Pressure effect	0.008
i=0.24 A/cm2	Temperature effect	0.0004
	Pressure effect	0.57
i=0.16 A/cm2	Temperature effect	0.0002
	Pressure effect	0.61
i=0.08 A/cm2	Temperature effect	0.0001
	Pressure effect	0.003

Table 6 – ANOVA analysis results

3.6.3   System efficiency

The system efficiency has been computed using the following equation:

$$\eta = \frac{\dot{Q}_{H2}*LHV}{P_{active}}$$

(18)

Where P_{active} is the active power required by the stack and by all the other components of the BoP.

The trend of the system efficiency as a function of the current density is very similar to that of the stack efficiency: as the current density increases, the system efficiency increases as well, and it shows higher values when the hydrogen is produced at 1 bar than when it is produced at 20 bar (see Figure 23).
In particular, when the cathodic pressure is equal to 1 bar, the maximum system efficiency is 51.5% and it is reached when the production level is the highest possible. Instead, the minimum efficiency is 37% and it is reached when the current density is equal to 0.08 A/cm2.
When the hydrogen is delivered at 20 bar, the maximum efficiency of 48.4% is obtained at a current density equal to 0.32 A/cm2. While, at 0.08 A/cm2 the minimum efficiency is measured, which is 28.7%.

Figure 22 shows the percentage points of difference between the stack efficiency and the system efficiency, for different values of current density and hydrogen pressure. It can be noted that the difference between the two efficiencies doesn't show any trend in respect of the current density or the pressure.

The biggest difference between the two parameters is reached at 0.32 A/cm2 and pressure equal to 20 bar, and it corresponds to 8.2%. Instead, it has been observed that the system efficiency is as close as possible to the stack efficiency when the current density is 0.24 A/cm2 and the cathodic pressure is set to 1 bar. The minimum difference results equal to 6.2%.

According to the literature, the system efficiency should be only 2 – 6 percentage points lower than the stack efficiency [24]. In addition, the difference between the two should be greater at low production rates and it should reach the minimum under rated conditions, because the components of the BoP are designed according to the nominal conditions.

These results have not been obtained, because the system design is not optimized, since this wasn't the goal of the experimental campaign. Despite this, the differences obtained between the 2 efficiencies don't differ a lot from the ones reported in the literature.
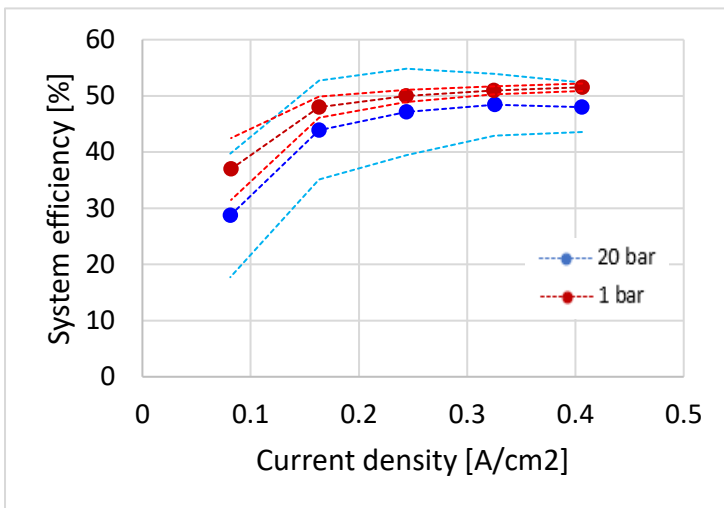
Figure 23 – System efficiency and its uncertainty VS current density for 2 levels of cathodic pressure
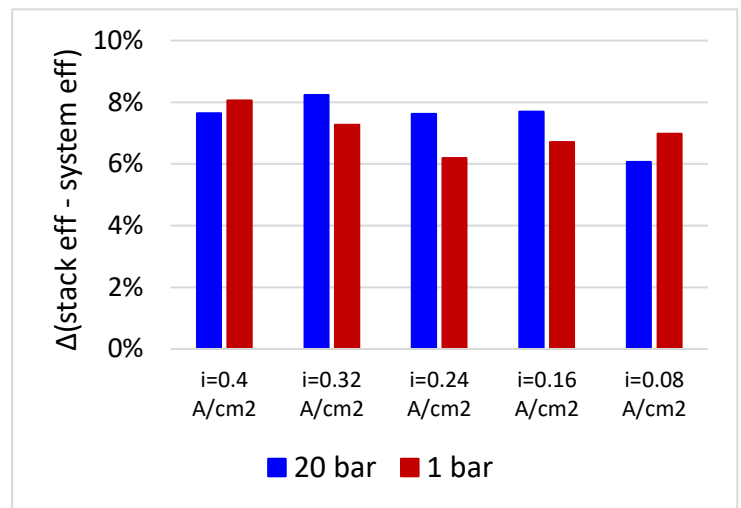
Figure 22 – Difference between system efficiency and stack efficiency

3.7   Final considerations

To conclude, it has been observed that to obtain the optimum working conditions of the electrolyzer, the following values must be set:

- hydrogen production setpoint equal to 500 l/h, which corresponds to a cell current density of 0.4 A/cm^2;
- hydrogen pressure setpoint equal to 1 bar.

In this operation mode, the stack efficiency reaches its maximum value of 58.8% and the real hydrogen flowrate results equal to 404.2 Nl/h. Instead, the overall system efficiency assumes the value of 50.9%. These results have been obtained for a cell temperature varying in a range of around 5°C (roughly 36°C – 41°C). While, in the electrolyzer nominal conditions, production setpoint equal to 500 Nl/h and cathodic pressure equal to 20 bar, the stack efficiency is lower, and it is equal to 55.6% and the system efficiency is 48%.

Furthermore, it has been noticed that the main cause of efficiency loss is due to the big difference between theoretical hydrogen production and the real production.

However, the measured efficiency values are in accordance with the ones referring to AEM technology available in the literature. IRENA, indeed, reports that the actual AEM electrolyzers show a stack electrical efficiency of around 51% – 65% at nominal current densities of 0.2-2 A/cm2, respectively [24]. Regarding the system efficiency, instead, it is around 48% - 58% at the two, aforementioned current densities [24].

3.7.1   Proposals to enhance electrolyzer performance

By analysing the electrolyzer operation and observing the tests' results, some suggestions that could lead to an improvement in the performance of the device have been identified.

First of all, a thermoregulation system could be added. In this way, the operating temperature is no more affected by the external conditions and the stack operates always at the temperature allowing it to reach the highest stack efficiency. Therefore, for each working condition, the power consumed by the cells is the minimum one. Nevertheless, the temperature control's impact on the overall efficiency must be carefully investigated and its integration in the system design must be optimized.

Another possible improvement is related to the cathodic pressure regulation. The back pressure valve could be replaced with a more sophisticated one, which allows a more regular and stable production of hydrogen.

Finally, since a quite low system efficiency was measured, an optimization of all components forming the electrolyzer would be necessary. To do so, the electrolyzer facility should be designed taking a whole-of-system perspective [24].

4 Model and simulation

4.1 Objectives

In these chapters, one application of the previously described AEM electrolyzer has been analysed.

In particular, it is carried out a techno-economic analysis on a system producing hydrogen from a renewable source and then delivering it to an industrial plant.

The objectives of this study were the following:

- Develop an algorithm for sizing the production system's components. The main sizing criterion has been the satisfaction of the hydrogen demand at each hour of the year.
- Conduct an economic analysis on the produced hydrogen cost. Another sizing criterion has been to obtain the lowest possible levelized cost of hydrogen (LCOH).
- Carry out a sensitivity analysis on the LCOH. Only the electrolyzer characteristics (efficiency and cost) have been modified.

Firstly, an off-grid system equipped with a dedicated photovoltaic field is modelled and then some considerations about its feasibility are drawn.

In the second place, other systems providing for the power grid support will be analysed.

Therefore, it is intended to compare different configurations producing hydrogen and then draw conclusions on which system is the more convenient.

4.2   Case study description

The case study concerns an industrial plant which requests hydrogen as fuel to partially substitute the use of gas, with the aim of gradually begin the decarbonization of its production.

In addition, the industry desires to be self-sustaining in the production of hydrogen and therefore, it is planning the construction of a photovoltaic field able to provide the needed electrical energy.

The industry is located in Puglia.
It is responsible for the agro-food processing. In particular, it produces oils and cereals intended for applications in food, pharmaceutical, cosmetic and energetic sectors.
The oils are obtained through several processes in series. First of all, the oilseeds are dried, then they are mechanically pressed, and the crude oil is extracted. Finally, if required, it undergoes to a further process to get refined vegetable oil.

The factory is equipped with a 4.4 MW gas cogeneration unit. The aim is to switch the fuel from NG to an NG-H2 blend (5% vol H_2).

This thesis work focuses on the modelling of a system able to satisfy the hydrogen demand of this industrial plant. Therefore, it deals only with the components before the cogeneration unit, which form the hydrogen production unit.

In the following paragraphs, the model of an off-grid hydrogen production unit will be developed.

It should be noticed that, although a real system is composed of several auxiliaries which affect the unit's dynamic response, only the four main components have been modelled.

Figure 24 shows the layout of the off-grid configuration.
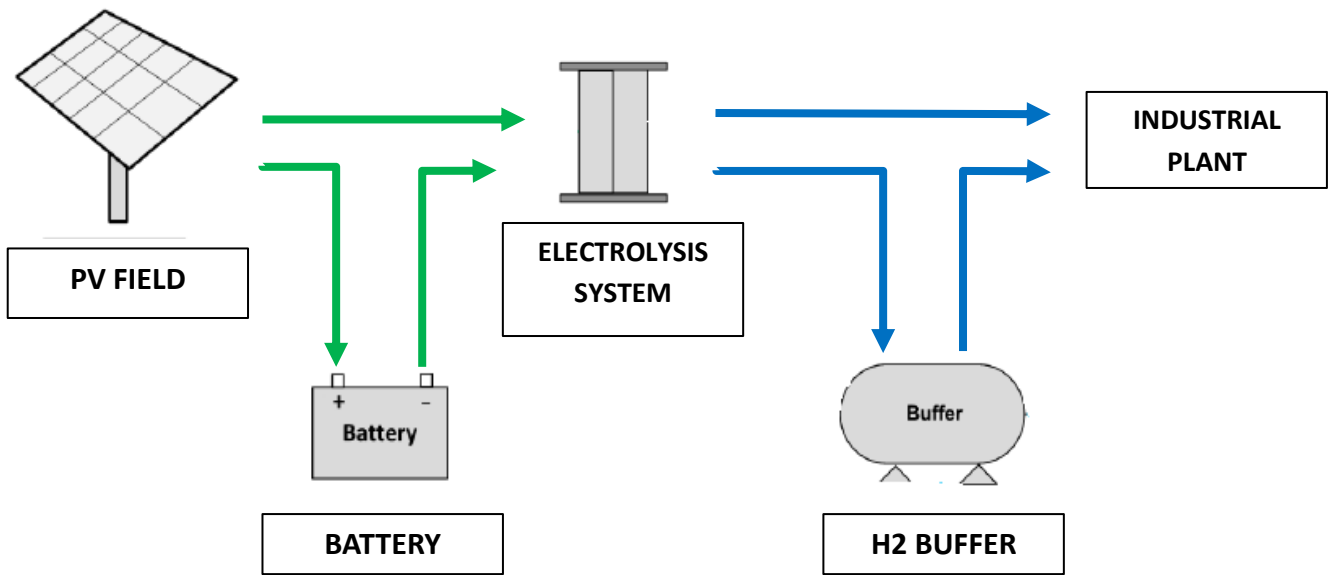
Figure 24 – Layout of the configuration with photovoltaic power supply and battery support

The main components represented are the photovoltaic field, which supplies the electrolyzer; the electrolysis system for producing hydrogen gas; two storage systems, a battery and a gas buffer, which are necessary to meet the hydrogen demand all hours of the year, even when there is no solar power available.

Concerning the battery usage policy, it is assumed as necessary in two main cases:

- if the electrical power required by the electrolyzer is greater than the power available from the photovoltaic field;
- if the electrical power provided by the PV field is greater than the power required by the electrolyzer.

Similarly, the buffer is used when:

- the hydrogen flowrate demanded by the plant is greater than the one produced by the electrolyzer;
- the electrolyzer produces more hydrogen than what is required by the industrial plant.

As it can be noted, the production systems is not equipped with a hydrogen compressor. In fact, it has been assumed that in the cogeneration unit, the hydrogen is not required at a specific pressure.

4.3 Assumptions

4.3.1 Photovoltaic field

The photovoltaic field has not been modelled, but real data of a solar park located in the area has been used. It is a large PV field, with a peak power of 6.5 MWp. The available data provide directly the produced electrical energy on an hourly basis for the year 2019.

Dealing with real data, decrements of energy production due to weather conditions, as clouds or rainy days, or possible not perfect conditions of the panels, as dirt and dust, are considered.

Then, these data are scaled depending on the size of the photovoltaic field needed for this case study. It is thus assumed that changing the size of the field, the trend of the produced energy in time remains the same.

Furthermore, the size of the PV field has been determined to cover at each hour the hydrogen demand, and thus, it has not been considered possible technical issues due to very large photovoltaic power installed, such as available space.

4.3.2 Battery

The battery bank is used as a daily electricity energy buffer, smoothing the photovoltaic output and reducing its intermittency.

It is a Li-ion battery bank and it is assumed to have the following characteristics [25]:
- charge efficiency = 0.92;
- discharge efficiency = 0.92;
- State Of Charge (SOC) limits = 0.2 -1.
The maximum and minimum battery State Of Charge must be controlled to protect the battery from being damaged, which happens in case of over-charging/discharging [26].
Furthermore, for sake of simplicity, it is assumed that the battery is able to instantaneously deliver electrical energy whenever is required.

4.3.3 Electrolysis system

The electrolyzer has not been mathematically modelled, but experimental data of the previously investigated AEM electrolyzer have been used.
However, the size of the real device is much smaller than what could be required in this application. Therefore, in the solving algorithm, whenever the required size has been found, the real device has been resized to fit it.

To do so, the main assumption made is that whatever the size is, the stack efficiency stays exactly equal to the one of the real electrolyzer, even though the latter is much smaller. In fact, the electrolysis unit has been considered as a parallel of many electrolyzers of size equal to the real one. In this way, the applied voltage is that of the small device, while the hydrogen production flowrate is proportional to the number of devices.

Since, as it was observed in chapter 3.6.3, the system design of the analysed electrolyzer is not optimized, the efficiency loss due to auxiliary components has been determined from literature.
In particular, it has been assumed that the system efficiency differs from the stack efficiency of 4 percentage points at all working conditions [24]. It's an approximation because, actually, the difference between the two efficiencies varies with the operating conditions: at low loads, it is higher than 4%, while, increasing the load conditions, the difference decreases to be lower than 4%.

Another assumption made regards the operation flexibility of the system. It is considered a load range of 0.05 − 1 [24]. It means that the electrolyzer cannot produce less than 5% of its rated production.
By means of the system efficiency, the load range has been converted into input power range. This implies that below a certain value, whatever input power is supplied to the electrolyzer, it is not able to produce hydrogen.
Finally, the equation relating the systems efficiency as a function of the ratio between actual input power and rated input power has been computed. In this way, once the electrolyzer's size (expressed as rated input power) is found, through this equation, the real device's data can be scaled.

It is also assumed that the electrolysis system instantaneously produces hydrogen whenever it is demanded.

4.3.4 Hydrogen buffer

The hydrogen buffer has been modelled as a tank able to store the surplus hydrogen and to immediately provide it when required.

The hydrogen tank level has to lie in a specific range for a correct operation: a minimum pressure is required to overcome downstream pressure drops and a maximum pressure for safety reasons [27].
Specifically, it is assumed that it can work in a pressure range of 3 − 20 bar [25]. Therefore, to ensure the minimum pressure, a certain quantity of hydrogen must always be present inside it.
It has been fixed the maximum quantity of storable hydrogen equal to 5 tons, which corresponds to the maximum limit in order not to be included under the Italian legislation 'Seveso'. In this way, no specific and strict rules must be followed and therefore, the hydrogen storage does not imply further costs, besides the buffer cost.

4.3.5 Hydrogen demand

Properties of hydrogen are different to those of natural gas and mixtures of hydrogen and natural gas have still other properties. This raises the problem that not all the existing natural gas infrastructure are suitable for utilizing such mixtures.

Since the existing cogeneration plant cannot be substituted with a new one designed specifically to work with hydrogen gas, it must work with a blending of natural gas and hydrogen. The maximum percentage of accepted hydrogen has been determined based on 'test results and regulatory limits for hydrogen admission into the existing natural gas infrastructure' [28].

It has been assumed to feed the cogeneration unit by a blending of 95 vol-% of natural gas and 5 vol-% of hydrogen. In this way, no modifications are to be made to the plant.

In this industry, the day is subdivided into 2 8-hours work shifts. Therefore, the cogeneration unit works 16 hours per day, in particular from 4 a.m. to 8 p.m.

The gas is requested all year, except during the closure periods of the plant, which are never more than 7 days. In fact, from the available data, it is possible to note that in 2019 the industry has closed for 5 days in August and for 3 in October, while in 2020 it has closed for 7 days in August.

The available data of the natural gas required by the cogeneration unit are referred to 2019. They are provided in hourly basis as standard volume of NG per hour. It has to be noticed that every H2 demand value has been increased by 5%, in order to obtain a hydrogen producing unit able to satisfy demand's peaks usually not seen.

Table 7 shows the average daily demand of gas when the cogeneration unit was only fed with natural gas and the actual hydrogen and natural gas daily demands.

Fuel	Average demand of NG (Nm3/day)	Average demand of H2 (Nm3/day)
100% NG	56576.5	/
Blending 95% NG – 5% H2	55444.9	1131.5

Table 7 – Average hydrogen demand

Looking at the hydrogen mass flow rate, the annual demand of hydrogen has turned out equal to **91.45 ton$_{H2}$/year**, and most of the time, the hydrogen request is between **18 kg/h** and **19.5 kg/h**.

In addition, the demand of hydrogen is around **6 -9 tons per month**, as represented in Figure 25.

It should be noted that the minimum request is measured in September, while the highest amount of hydrogen is required during December and January. This will comport some components' sizing issues because of the lowest solar energy availability during those months.
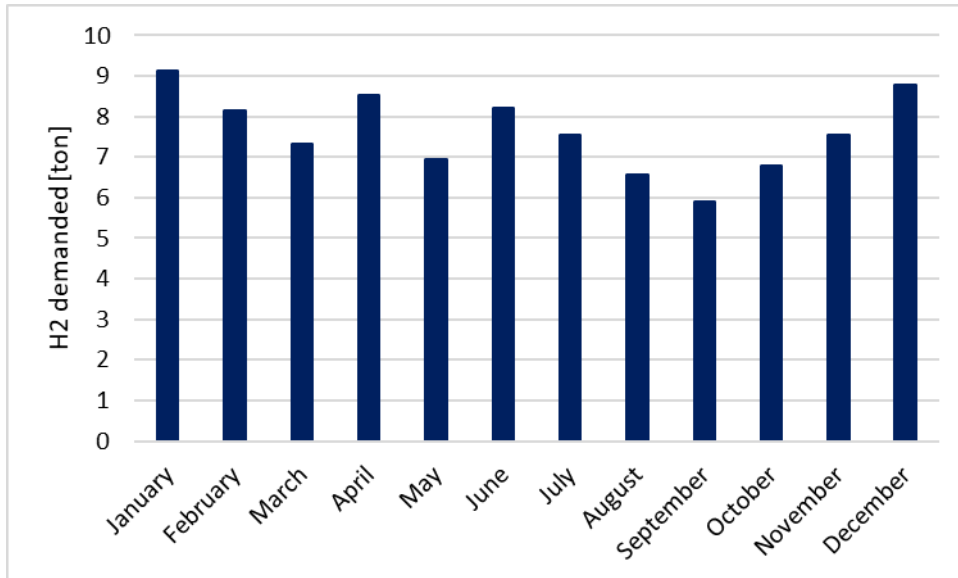

Figure 25 – Monthly demand for hydrogen

Finally, an example of hourly hydrogen demand during a typical day is represented in Figure 25.
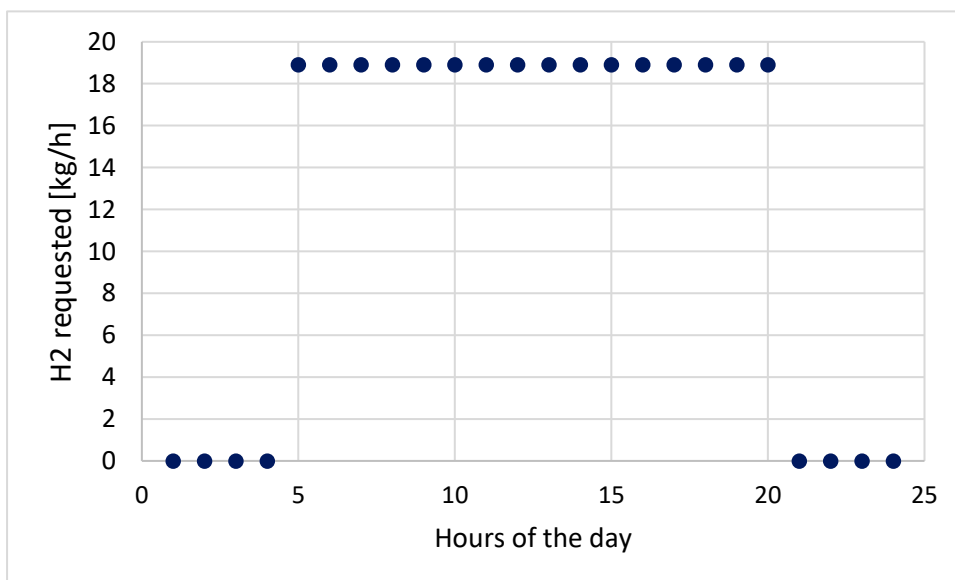

Figure 26 – Hydrogen requested during a typical working day

As already mentioned, since the working day starts at 5 a.m. and ends at 8 p.m., during the other hours the request of gas is nil. Furthermore, the hydrogen demand is virtually constant.

4.4   System components' sizing

The model has been developed using the MATLAB environment.

Two main criteria have been adopted and consequently, two steps have been followed to select the components sizes:

1. Technical criterion: satisfied hydrogen demand. The hydrogen demanded by the industrial plant must be met at all hours of the year.
   In this step many possible system configurations, in terms of components' sizes, are determined.
2. Economic criterion: levelized cost of hydrogen (LCOH). The LCOH has to be minimized.
   In this step the configuration, among those found previously, which allow to obtain the lowest LCOH has been identified.

Starting from the first step, the algorithm implemented is reported in the following pages.

The model approach is bottom-up: for each time step, it starts looking at the hydrogen demanded by the industrial plant and the hydrogen needed to completely fill the buffer. Then the input power needed by the electrolyzer to produce that specific amount of gas is read.

Form this point forward, this just mentioned power will be referred to as the *required input power.*

Priority of operation is given to the battery. If the available photovoltaic energy is not sufficient to meet the hydrogen demand, firstly, the battery is required to supply the missing energy. Only when it exceeds its SOC limits, the hydrogen buffer participation is required.

The hydrogen buffer, indeed, works as a hydrogen stock, usable in case of absence of hydrogen production because of lack of the required input power to the electrolyzer or any components failure, avoiding the unsatisfaction of the industrial plant request. For this reason, the electrolyzer aims at filling as much as possible the buffer, other than producing enough hydrogen to meet the demand.

At this point three cases are outlined:

1) (Figure 27). The available power, coming from the photovoltaic plant and/or from the battery, satisfies totally or partially the required input power.
   The electrolyzer production meets the hydrogen demand and, if surplus hydrogen is produced, it will be stored into the hydrogen buffer.
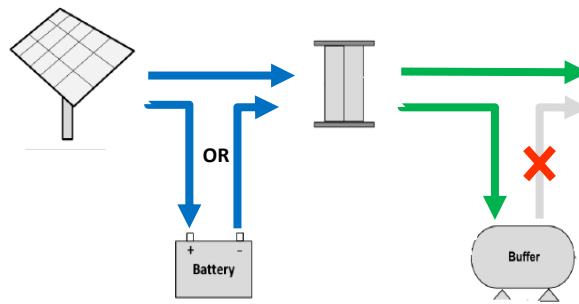
Figure 27 – Representation of the hydrogen production unit – CASE 1

2) (Figure 28) The required input power is not satisfied. However, the available power, coming from the photovoltaic panels and/or from the battery, is greater than the minimum input power acceptable by the electrolyzer.

Or the required input power is greater than the electrolyzer maximum acceptable power.

The electrolyzer produces hydrogen and if the amount of gas produced is greater than the demand, surplus is stored into the buffer. Otherwise, the deficit hydrogen is supplied by the buffer.
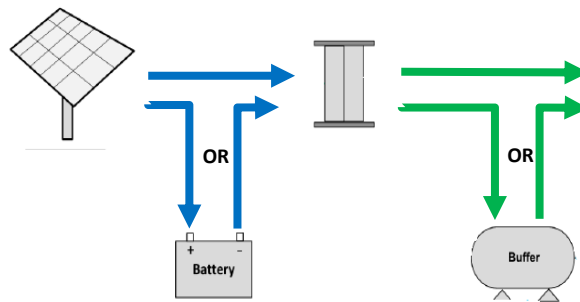
Figure 28 - Representation of the hydrogen production unit – CASE 2

3) (Figure 29) The required input power is smaller than the minimum input power acceptable by the electrolyzer. Or the available input power, coming from photovoltaic panels and/or from the battery, is smaller than the minimum input power acceptable by the electrolyzer.

The electrolyzer doesn't work, and the hydrogen demand is totally satisfied by the buffer.
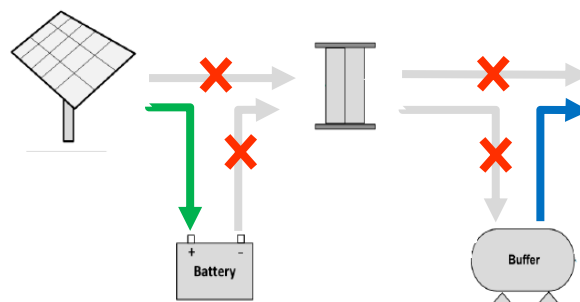
Figure 29 - Representation of the hydrogen production unit – CASE 3

In all 3 cases, whenever some energy produced by the photovoltaic field is not used, it is stored into the battery bank until it reaches its highest state of charge. Otherwise, the remaining solar energy is curtailed.

The simulation timeframe which has been adopted is reported in Table 8.

Beginning of simulation	18th August 2018 at 00:00
End of simulation	17th August 2019 at 23:00
Simulation time step	1 hour

Table 8 – Simulation timeframe

The simulation starts when the battery is completely charged, and the hydrogen buffer is completely full. Therefore, before the beginning of the simulation, it is considered that the production unit works without supplying the industrial plant until these conditions are reached.

To obtain possible system configurations, an iterative method has been followed, by trying different combinations of photovoltaic field, battery bank, electrolyzer and hydrogen buffer sizes.

Table 9 reports which characteristic dimension has been considered for each component and how much it has been modified at each simulation.

COMPONENT	CHARACTERISTIC DIMENSION	STEP
Photovoltaic field	Peak power	10 kWp
Battery bank	Capacity	5 kWh
Electrolysis unit	Rated input power	5 kW
Hydrogen buffer	Mass of hydrogen storable	5 kg

Table 9 – Characteristic dimensions of each component

4.4.1 Results

By observing some possible configurations, it has been noted that all the system components are related.

By keeping constant 2 components and varying the other 2, the following relations have been observed:

- As the photovoltaic farm's size increases, it can be used a smaller battery bank;
- With a bigger hydrogen buffer, a smaller electrolyzer can be used;
- Increasing the electrolyzer's size, the photovoltaic field can be smaller;
- With a bigger photovoltaic field, a smaller buffer is needed;
- As the buffer's size increases, a smaller battery can be used.

By post-processing the simulation results, some useful performance indicators have been calculated on a yearly basis:

- Electrolyzer capacity factor (CF):

$$CF = \frac{Q_{H2,produced|year}}{Q_{H2,rated|year}} * 100 \tag{19}$$

It expresses the percentage of the electrolyzer's actual generation output over what is capable of generating at rated conditions, on a yearly basis.

- Surplus photovoltaic power to curtailment (PCi):

$$PC = \frac{P_{pv,curtailed}}{P_{pv,total}} * 100 \tag{20}$$

It expresses the percentage of the curtailed power over the total power produced by the photovoltaic field.

- Electrolyzer power request directly covered by photovoltaic field production (KPI1):

$$KPI1 = \frac{P_{pv \rightarrow el}}{P_{el,total}} * 100 \tag{21}$$

It expresses the percentage of the power directly provided by PV farm over the total power required by the electrolyzer.

- Hydrogen demand directly covered by electrolyzer production (KPI2):

$$KPI2 = \frac{Q_{H2,el \rightarrow demand}}{Q_{H2,demanded}} * 100 \qquad (22)$$

It expresses the percentage of the hydrogen demand directly covered by the electrolyzer production.

- Hydrogen demand covered by buffer (KPI3):

$$KPI3 = \frac{Q_{H2,buffer \rightarrow demand}}{Q_{H2,demanded}} * 100 \qquad (23)$$

It expresses the percentage of the hydrogen demand covered by the hydrogen stored into the buffer.

Three possible system configurations are reported below together with graphs showing the energy supplied to the electrolyzer and the hydrogen provided to the industrial plant.

Moreover, also figures showing the annual trends of the hydrogen buffer and battery state of charges are reported.

1) System n.1.

The electrolyzer rated production has been fixed equal to the most frequent hydrogen demand, which is between 17.6 – 19.1 kg/h. Consequently, the rated input power has been fixed to 1210 kW.

The sizes of the other components have been determined by fulfilling the technical criterion of satisfaction of the hydrogen demand all hours of the year.
Therefore, the following configuration has been obtained:

	PV field	Battery bank	Electrolyzer	H2 buffer
System n.1	9.5 MWp	23.28 MWh	1210 kW	4.995 ton

Table 10 - Main features of system configuration n. 1
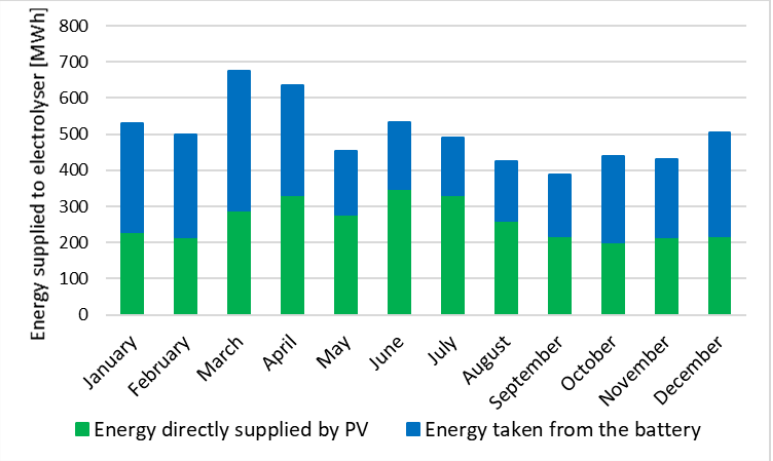
Figure 31 – Monthly energy supplied to the electrolyzer – System n.1   *Figure 30 - Monthly hydrogen supplied to the industrial plant – System n.1*
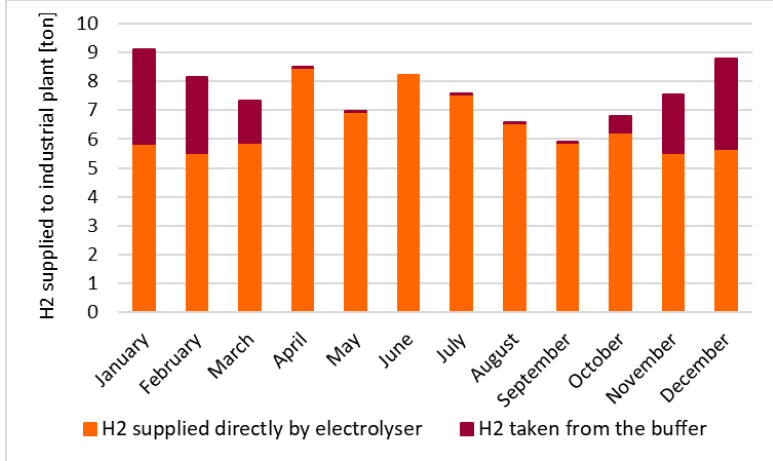
Figure 31 shows that, most of the months, the electrolyzer is supplied, on average, with 50% of energy coming directly from the photovoltaic field and 50% of energy taken from the battery. During the summer months, especially on June and July, because of the higher solar energy availability, the PV plant provides almost 70% of the energy requested by the electrolyzer.

Furthermore, as visible in Figure 30, from April to September, the energy supplied to the electrolyzer allows it to almost fulfil the hydrogen demand completely without needing of discharging the hydrogen buffer. Instead, during the winter months, when less photovoltaic energy is available and the battery isn't able to supply all the energy needed by the electrolyzer to satisfy the demand, 30% of the monthly demand is covered by the gas in the tank.
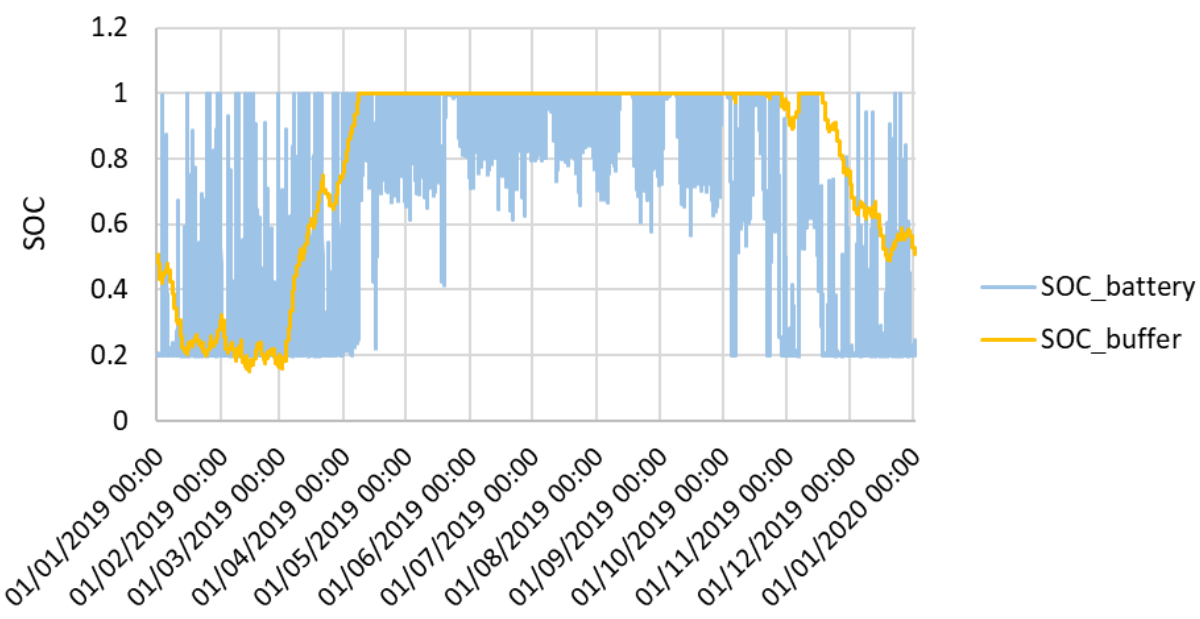
Figure 32 – Buffer and battery SOCs – system n. 1

Figure 32 shows the battery and buffer State Of Charges. Both the storages are exploited in all their SOC range. It can be noted that from April to the middle of October, the buffer remains always full. Instead, its level of charge decreases a lot during the other months.

Except during the summer period, from June to September, the battery continuously undergoes to charging and discharging cycles.

2) System n. 2.

The battery has been sized in order to contain all the energy required by the electrolyzer during the two consecutive days with the lowest available solar power and highest hydrogen demand. During these days, the 1st and 2nd of January, the total hydrogen demand corresponds to 586.9 kg, and therefore, it has been computed that the capacity of the battery has to be around 50 MWh.

The other components have been determined by fulfilling the satisfaction criterion:

	PV field	Battery bank	Electrolyzer	H2 buffer
System n.2	9.05 MWp	49.325 MWh	2550 kW	4.995 ton

Table 11 - Main features of system configuration 2
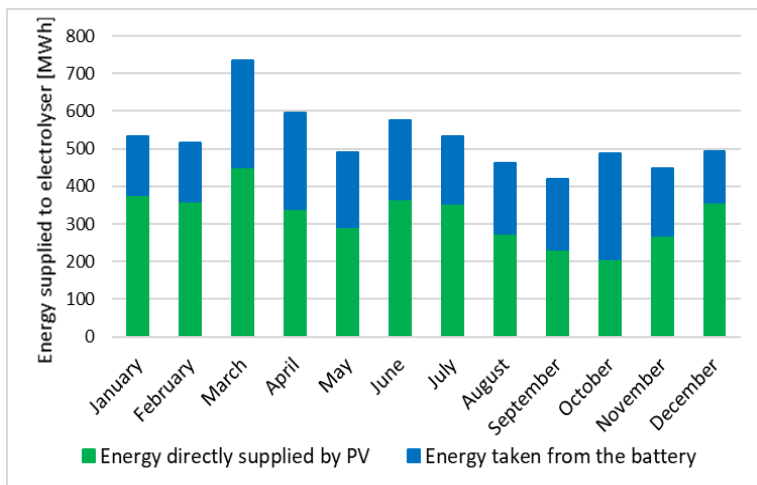
Figure 34 - Monthly energy supplied to the electrolyzer – System n.2
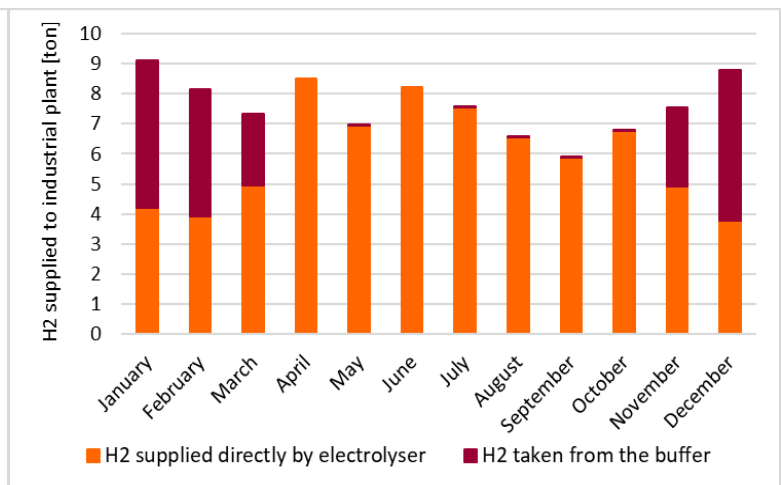
Figure 33 - Monthly hydrogen supplied to the industrial plant – System n.2

Figure 34 shows that during the winter months only 30% - 40% of the required power is supplied by the battery, since it is almost totally discharged. In the other months, instead, the battery has a lot of available energy, however, because of the high solar availability, most of the required energy is provided by the PV field.

In Figure 33 is visible that from April to October, one month more than in system n.1, the buffer isn't discharged at all. This is due to the large capacity of the battery: it is able to provide all the required energy to the electrolyzer to completely satisfy the hydrogen demand.

During the other months, some hydrogen from the tank must be taken, because the battery is at its minimum state of charge and thus it isn't able to feed the electrolyzer as required.
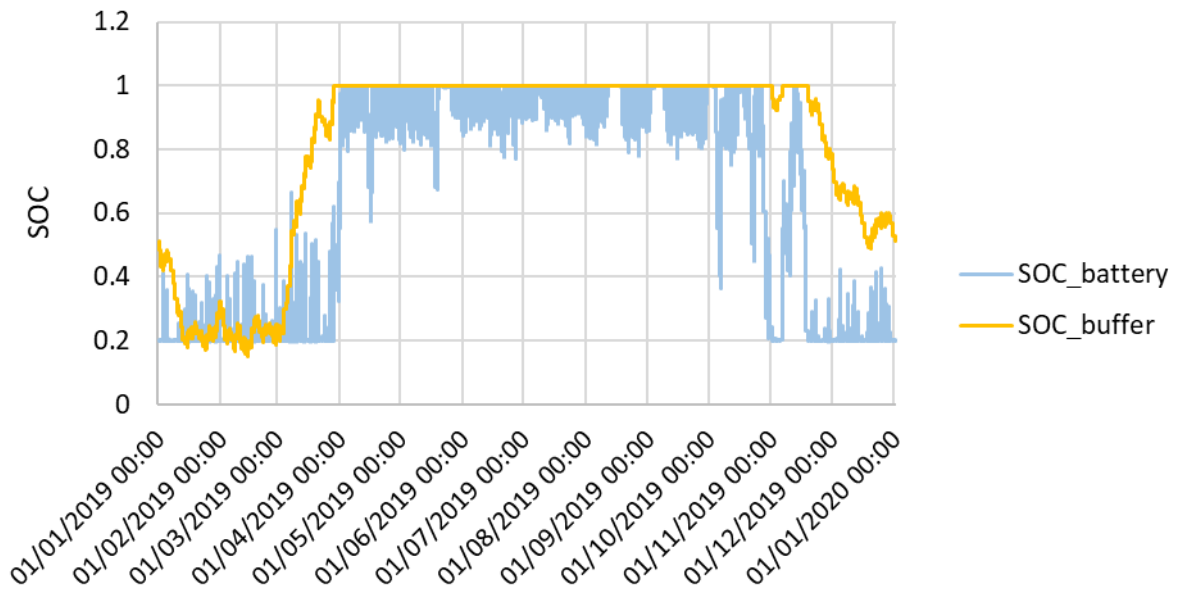
Figure 35 - Buffer and battery SOCs – system n. 2

Being the buffer of the same size of the previous one, it is visible in Figure 35 that its SOC profile is very similar.

The battery size is bigger than before and indeed, it is exploited less. In particular, it is fully recharged only during the spring – summer months, while it is totally discharged in the less sunny months.

3)   System n. 3.

This configuration allows to obtain the lowest LCOH. It has been obtained by iteratively simulating different components sizes and verifying the accomplishment simultaneously of both the hydrogen demand and the reduction of the LCOH.

	PV field	Battery bank	Electrolyzer	H2 buffer
System n.3	9.5 MWp	795 kWh	4995 kW	4.995 ton

*Table 12 - Main features of system configuration 3*
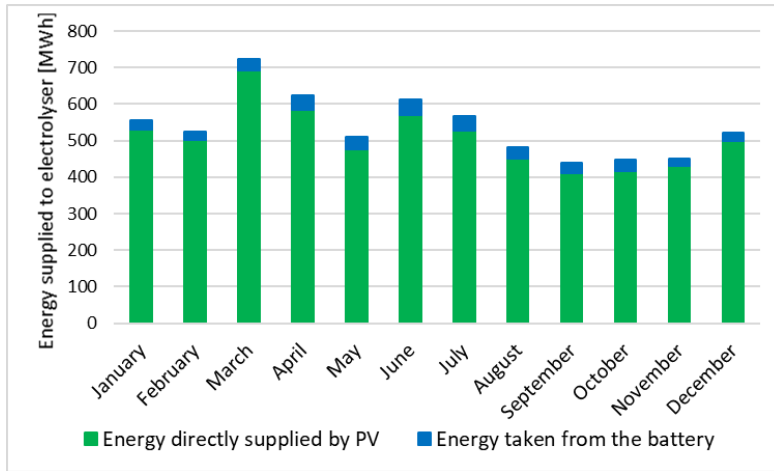
Figure 37 – Monthly energy supplied to the electrolyzer – System n.3
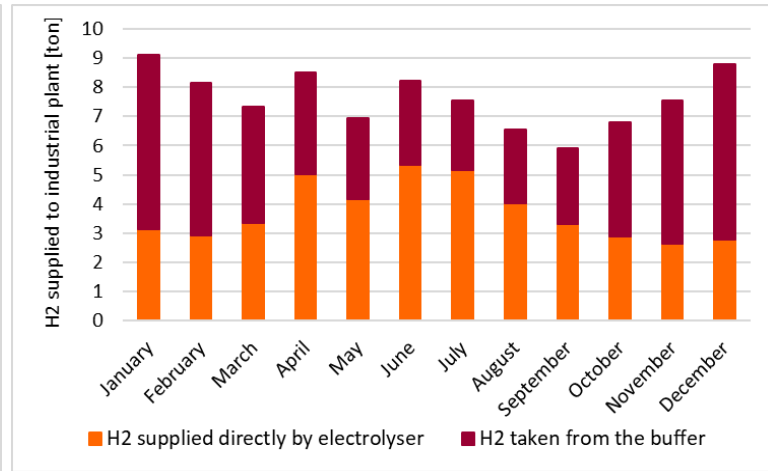
Figure 36 – Monthly hydrogen supplied to the industrial plant – System n.3

Figure 37 shows that, being the battery much smaller than before, around 95% of the electrolyzer input energy is directly supplied by the photovoltaic field, all months of the year.

However, on average, the energy supplied to the electrolyzer is never enough to fulfil the hydrogen demand all year. Therefore, as shown in Figure 36, to satisfy the hydrogen request, gas from the tank must be taken.

As expect, since the PV available energy is greater during the months of June, July and August, only around 35% of the needed hydrogen must be provided by the buffer.
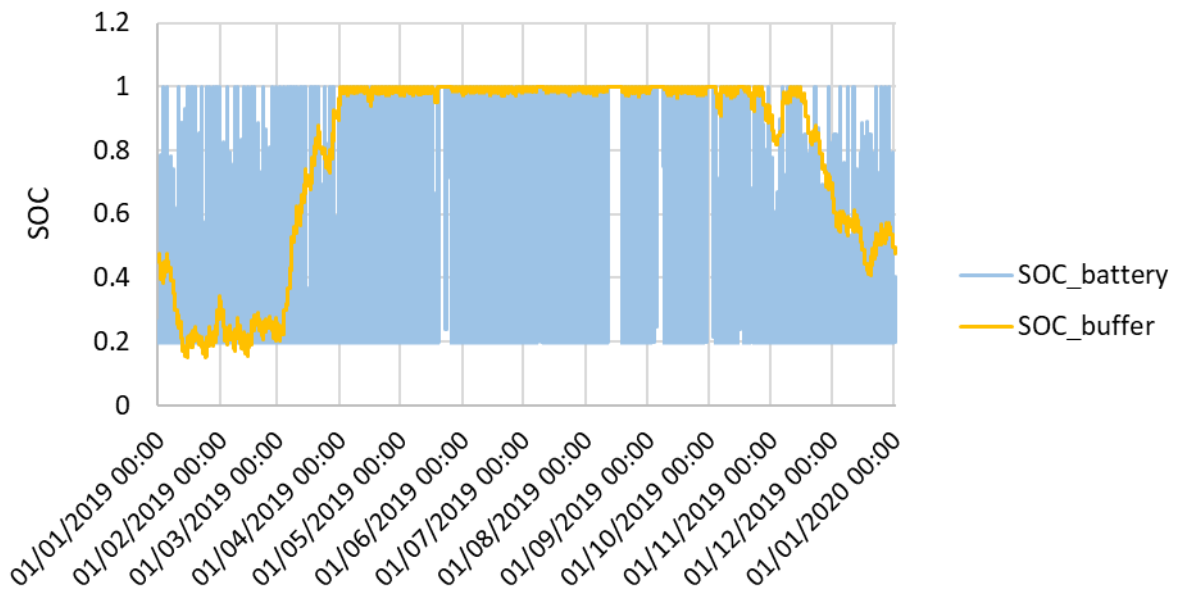
Figure 38 - Buffer and battery SOCs – system n. 3

In Figure 38 it can be noted that the hydrogen buffer SOC profile is very similar to the one of the other systems.

Instead, being the battery smaller, it is used much more than in the previous configurations: all months of the year it continuously undergoes to charging-discharging cycles.

4.4.2 Comments

In all previously analysed systems, the PV field was characterized by a large size. It has been observed that also with a battery of around 50 MWh capacity, to satisfy the hydrogen demand it was still required a huge PV plant of around 9 MWp.

This is due to the fact that during the winter months, especially from the middle of November to the first days of January, the intensity of the solar power is low, and in addition, it is available on average just from 7 a.m. to 3 p.m.. On the contrary, during these months the hydrogen demand is greater compared to the summer months. It is always 16 hours per day and constant around 18.5 kg/h in January and 18 kg/h in December.

Due to this reason, besides the big photovoltaic field, also very big storage devices are needed to be able to satisfy the industrial request of those days.

If the hydrogen demand had been lower in the months of December and January, surely the necessary photovoltaic field would have been lower.

The graphs, representing the states of charge of the storage devices, show as they have been exploited in all their operating ranges. This observation highlights the fact that they are not oversized and that both their presence is necessary.

Moreover, the adopted strategy is visible: the battery bank is exploited much more than the hydrogen buffer. To meet the hydrogen demand, if the PV field doesn't supply enough energy, the deficit energy is requested to the battery. Only when the battery cannot fulfil the requirement, hydrogen from the buffer is used. Otherwise, the buffer is used in order to have available hydrogen in case of need.

Furthermore, in all three configurations, it was visible as, in the central months of the year, from April to October, the hydrogen buffer was basically not used and the battery bank, when of big size, was used less than in other months. This is due to the big size of the photovoltaic field and to the high solar availability during these months. The PV panels are able to provide all the required power to the electrolyzer, almost without the need for storage systems.

In Table 13 the main indicators of each system are reported.

	PV power curtailment	Electrolyzer capacity factor	Required power directly supplied by PV (KPI1)	H2 demand directly covered by electrolyzer production (KPI2)	H2 demand covered by gas stored in buffer KPI3
System 1	43.7%	87.3%	50.2%	85.6%	14.4%
System 2	38.7%	50.1%	60.5%	78.9%	21.1%
System 3	41.3%	37.5%	94.2%	48.9%	51.1%

Table 13 – Comparison of the main indicators of the three systems

In all configurations, around 40% of the total available photovoltaic power is curtailed.

It may seem that the photovoltaic plants have been oversized, since the percentage of surplus power curtailment is not negligible. However, as already observed, these big PV plants are needed to guarantee the accomplishment of the hydrogen demand also during the winter months.

By looking at the results, it has been noted that as the electrolyzer size decreases, its capacity factor increases. In fact, the smaller is the electrolyzer, the more it works at its maximum capacity. Decreasing the device's rated power from 2550 kW (system n.2) to 1210 kW (system n.1), indeed, its capacity factor passes from 50% to 87%.

As previously said, most of the time the hydrogen demand is equal to 17-19 kg/h, which corresponds to the electrolyzer rated production of system n.1. This means that this electrolyzer works most of the time at its rated conditions and therefore that it reasonable observing a very high-capacity factor.

KPI1, which represents the percentage of the required power directly covered by PV, reaches the value of 94% in system n.3. In this configuration, indeed, the capacity of the battery is very small compared to the one of the other systems.

Looking at KPI2, it is notable that the highest value corresponds to system n.1. In this configuration the electrolyzer directly provides around 86% of the hydrogen demand, because, as said, its rated production corresponds to the hydrogen requested.

The percentage of hydrogen demand directly covered by the electrolyzer production decreases as the electrolyzer size increases. Bigger is the device, indeed, more times happens that its minimum input power is greater than the available power and therefore, it cannot work, and the hydrogen demand is satisfied by the gas stored in the buffer (decrement of KPI2 and increment of KPI3).

4.5 Economic analysis

A brief economic assessment has been carried to select the best system configuration among those possible. The selection criterium has been the lowest levelized cost of hydrogen (LCOH).

The LCOH expresses the overall cost to produce a kilogram of hydrogen. It takes into account the initial investment cost due to plant construction and all the management costs over the entire lifetime.
It can be computed through the formula expressed in equation (24) [29].

$$LCOH = \frac{Total\ cost\ (€)}{H_2\ annual\ production\ (kg)} \qquad (24)$$

The total cost consists of the sum of 3 terms: the annual capital repayment, the annualized replacement cost and the annual operation and maintenance cost.

- Annual capital repayment: $C_{inv,a}$ [29].

$$C_{inv,a} = \frac{i*(1+i)^n}{(1+i)^n-1} * C_{inv} \qquad (25)$$

It considers the total plant capital investment costs (C_{inv}), the plant lifetime (n) and the nominal interest rate (i).

- Annualized replacement cost: $C_{rep,a}$ [29].

$$C_{rep,a} = \frac{i*(1+i)^n}{(1+i)^n-1} * \frac{C_{rep}}{(1+i)^t} \qquad (26)$$

Where, C_{rep} is the replacement cost

t is the considered year.

It represents the annual cost rate to replace all the components and parts that wear out during the plant lifetime.

- Operation and maintenance cost: $C_{o\&m}$ [29].

It is calculated on yearly basis, and it represents the cost to guarantee the normal operation and maintenance of the plant.

4.5.1 Assumptions

The specific costs of the main components are shown in Table 14.

Component	Investment cost	Replacement cost	Replacement time	O&M cost	Reference
PV field	780 €/kWp	80 €/kWp	10 y	12 €/kWp	[30]- [25]
Li-ion battery	550 €/kWh	550 €/kWh	10 y	/	[31]
AEM electrolyzer	1200 €/kW	35% Cinv	40000 h	2% Cinv	[15] - [30] - [32]- [14]
Hydrogen buffer (20 bar)	353 €/kg	353 €/kg	20 y	3% Cinv	[31]

Table 14 – Specific costs of the main components of the system

As the AEM electrolyzer has not been used yet on a commercial scale, no data about its replacement cost and its operation and maintenance costs are available in the literature. Therefore, it has been assumed that they are similar to the ones of the already existing technologies, alkaline and PEM. Then, by looking at different studies, a replacement cost equal to 35% of the investment cost and a O&M cost equal to 2% of investment cost have been considered.
The investment cost and replacement time, instead, have been provided by Edison.

Considering the battery component, it has not been taken into account the economic impact due to its relevant usage. In fact, it has been considered that the continuous charging-discharging of the battery doesn't accelerate its degradation process. [27]

Other hypotheses regarding the interest rate (i) and the plant lifetime (n) are reported in Table 15.

Parameter	Value
Nominal interest rate	3% [29]
Plant lifetime	25 years

Table 15 – Economic hypothesis

4.5.2   Results

The levelized costs of hydrogen obtained for the 3 configurations are shown in Table 16.

Configuration n.	PV field [MWp]	Battery [kWh]	Electrolyzer [kW]	H2 buffer [ton]	LCOH [€/kg]
1	9.5	23280	1210	4.995	**24.08**
2	9.05	49325	2550	4.995	**41.07**
3	9.5	795	4995	4.995	**15.02**

Table 16 – LCOH for the 3 configurations

The system with the smallest battery and bigger electrolyzer's size is the most convenient: the hydrogen cost is around 15.02 €/kg.

Instead, despite in configuration n.2 both the photovoltaic field and the electrolyzer have a lower size than the previous system, the LCOH is higher. The reason is due to the size of the battery, which is two and sixty times greater than the one of configuration n.1 and n.3, respectively.

Finally, it can be seen that in configuration n.1 the hydrogen costs more than in configuration n.3, around 24 €/kg. This is only due to the higher capacity of the battery. The electrolysis system, indeed, is smaller and both the hydrogen buffer and the PV field have the same dimensions.

Therefore, it would appear that the battery size has a very big impact on the final hydrogen cost. This observation will be confirmed by the results shown below.

Figure 39 shows the contribution of the investment cost, replacement cost and operation and maintenance cost to the total system cost.
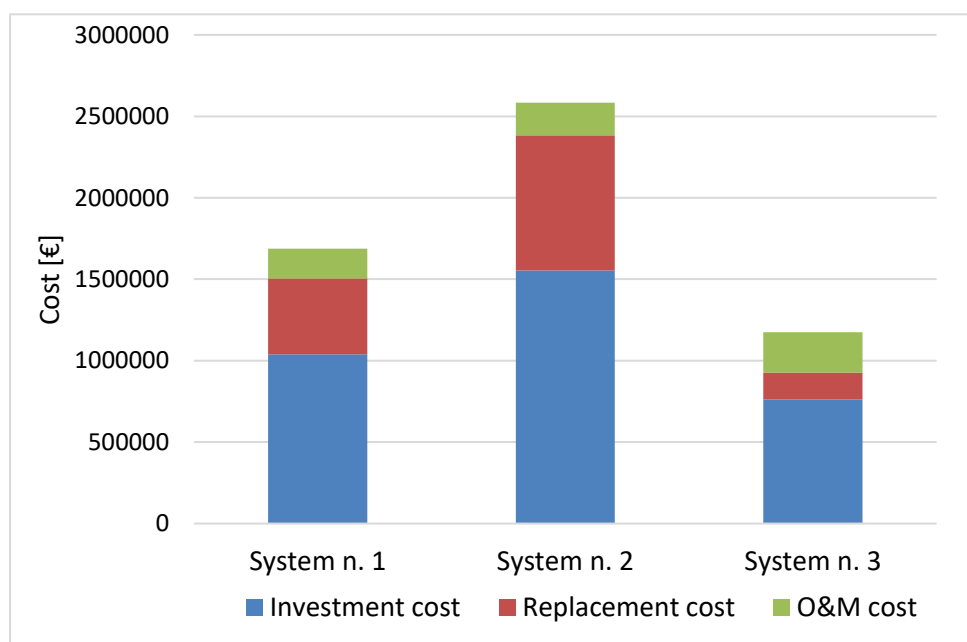
Figure 39 - Investment cost, replacement cost and O&M cost compared to the overall system cost

As expected, the highest overall cost is that of configuration n.2, while the lowest one is that of configuration n.3.

In all three systems, the investment cost is the most impacting and it makes up about 60% of the overall cost. In particular, for system n.1 is 61%, while for system n.2 is 60% and for system n.3 is 65% of the total cost. Therefore, the investment cost is the parameter which more affect the LCOH.

In Figure 40, the investment cost is broken down to better visualize the most impacting component.
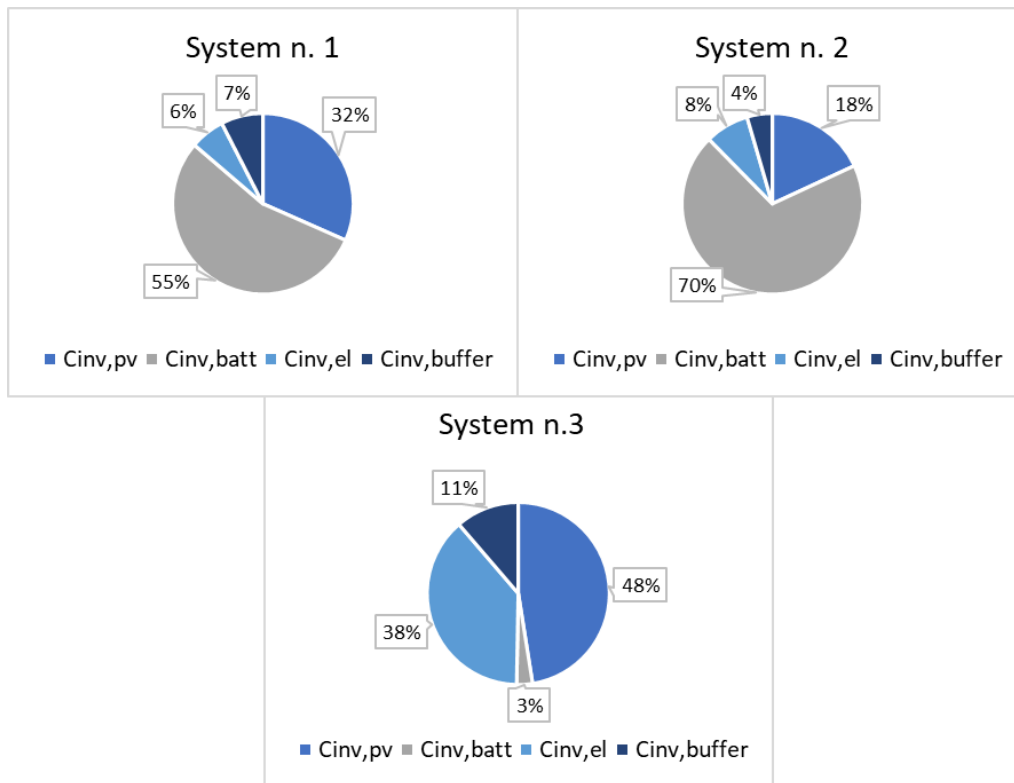
Figure 40 – Influence of the components costs on the total investment cost

In all three systems the buffer is characterized by a very big capacity, equal to 4.95 tons of hydrogen. However, its cost represents only around 10% of the total investment cost, because of its low specific cost, as reported in Table 14.

The costs of the photovoltaic fields have a considerable hand in the overall costs. This is related to their big dimensions and not to their high specific costs.

In configuration n.1, 55% of the total cost is due to the battery cost. Despite being the PV farm very big, a battery bank of a total capacity equal to 23 MWh is the main responsible of a so high investment cost.

In configuration n.2, the most impacting component is the battery as well. It is responsible of more than half of the total investment cost, exactly 70%.

Finally, in configuration n.3, since the battery is very small, its cost is almost negligible compared to the ones of the other components. Instead, the big photovoltaic field and electrolyzer have the greatest impact on the total investment cost, they correspond to 48% and 38%, respectively.

Therefore, as observed, the more impacting components are the battery and the PV field. Since, as discussed in chapter 4.4.2, it's not possible to reduce a lot the PV size, to obtain a low levelized cost of hydrogen, it's necessary to have a battery of small size, as configuration n.3 shows.

Consequently, being a sizing criterion of the hydrogen production unit the minimization of the LCOH, configuration n.3 has been selected for the case study. By simulating many combinations of components, indeed, the lowest cost of hydrogen has been obtained with these sizes.

In addition, instead of curtailing the excess electricity produced by PV, it has been considered to sell it to the grid. For sake of simplicity, it has been assumed an average remuneration electricity price of 50 €/MWh [33]. Therefore, considering the revenues from electricity sale, the levelized cost of hydrogen is reduced from **15.02 €/kg** to **12.51 €/kg**.

4.6 Sensitivity analysis

Since the case study concerns an application of the AEM electrolyzer, the sensitivity analysis focuses on this component.

Firstly, a sensitivity analysis on the LCOH has been carried out, by varying the capital cost and replacement time of the electrolysis unit.
Secondly, the efficiency of the electrolyzer has been changed to see how it affects the overall system and the hydrogen cost.

- VARIATION OF ELECTROLYZER'S CAPITAL COST AND REPLACEMENT TIME.

According to the European Commission's Fuel Cells and Hydrogen Joint Undertaking (FCH JU) target, in 2030 the capital cost of an AEM electrolyzer will be 450 €/kWe and the lifetime of the stack will be 67000 operating hours.

Therefore, the LCOH of the selected configuration has been computed for three different investment costs (1200 – 825 – 450 €/kWe) and for three different replacement times (40000 – 54000 – 67000 operating hours).

As Figure 41 shows, decreasing the investment cost and increasing the replacement time, the cost of hydrogen decreases. In particular, reducing the capital cost of 375 €, the LCOH decreases of 1.87 €/kg.
It can be noted that, passing from the actual scenario to a future scenario, where the electrolyzer cost is 450€ and its lifetime is 67000 hours, the hydrogen cost passes from 12.51 €/kg to 8.69 €/kg.
Therefore, keeping the same system configuration and only changing some electrolyzer parameters, the LCOH decreases of around 3.8 €/kg.
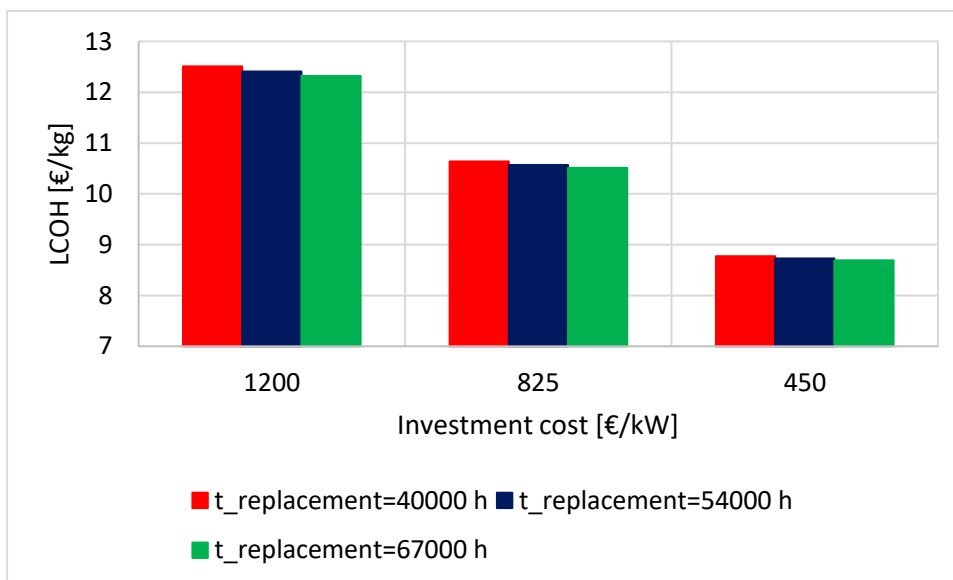
Figure 41 – Different LCOHs due to different electrolyzer investment costs and replacement times.

- VARIATION OF THE ELECTROLYZER EFFICIENCY.

A future target of the AEM electrolyzer is to achieve in 2050 a system efficiency higher than 74% [24]. Therefore, the simulation has been carried out considering this so high efficiency for the electrolysis unit. Three possible configurations have been modelled and compared to the three systems found previously for the less efficient AEM electrolyzer.

1) System n.1

	PV field [MWp]	Battery [kWh]	Electrolyzer [kW]	H2 buffer [kg]	LCOH [€/kg]	Electrolyzer capacity factor	PV power curtailment
Less efficient AEM electrolyzer	9.5	23280	**1210**	4995	24.08	87.3%	43.7%
More efficient AEM electrolyzer	7.5	9760	**1210**	4995	14.61	70.8%	48.6%

Table 17 – Comparison between a system provided with the less efficient AEM electrolyzer and one with a more efficient AEM electrolyzer – System n.1

Keeping constant the electrolyzer rated production, the sizes of the other components have been obtained by assuring the satisfaction of the hydrogen demand all year.

It can be noted that, since the electrolyzer is more efficient and thus requires less energy to produce the same amount of hydrogen, both a smaller photovoltaic field and a smaller battery is required. Consequently, the LCOH decreases by around 10 €/kg$_{H2}$.

Looking at the electrolyzer capacity factor, in the second case it is a bit lower. For the more efficient device, indeed, the size which corresponds to a rated production equal to the most frequent demand is lower and it is around 800 kW.

Finally, in both cases the PV power curtailment is not negligible.

2) System n.2

	PV field [MWp]	Battery [kWh]	Electrolyzer [kW]	H2 buffer [kg]	LCOH [€/kg]	Electrolyzer capacity factor	PV power curtailment
Less efficient AEM electrolyzer	9.05	**49325**	2550	4995	41.07	50.1%	38.7%
More efficient AEM electrolyzer	6.43	**49325**	1640	4995	38.25	54.6%	38.6%

Table 18 - Comparison between a system provided with the less efficient AEM electrolyzer and one with a more efficient AEM electrolyzer – System n.2

In this system, the battery capacity is assumed equal to the one of the system having the less efficient electrolyzer.

It can be observed that the needed photovoltaic field is smaller of about 2.5 MWp when the electrolyzer is more efficient. Due to this reason and to the smaller electrolyzer size, the LCOH decreases by around 3 €/kg$_{H2}$. Finally, both the electrolyzer capacity factor and the PV power curtailment are very similar in the two cases.

3) System n.3

	PV field [MWp]	Battery [kWh]	Electrolyzer [kW]	H2 buffer [kg]	LCOH [€/kg]	Electrolyzer capacity factor	PV power curtailment
Less efficient AEM electrolyzer	9.5	795	4995	4995	**15.02**	37.5%	41.3%
More efficient AEM electrolyzer	7.5	260	3000	4995	**11.02**	43.9%	48.4%

Table 19 - Comparison between a system provided with the less efficient AEM electrolyzer and one with a more efficient AEM electrolyzer – System n.3

These configurations have been obtained by reducing as much as possible the levelized cost of hydrogen.

In the system provided with the more efficient AEM electrolyzer, both the PV field, the battery and the electrolyzer have a smaller size compared to the less efficient system. As a consequence, the levelized cost of hydrogen decreases by 4€/kg$_{H2}$, being equal to 11.02 €/kg$_{H2}$.

Furthermore, it has been computed that, being the capacity of the battery very small, 97% of the energy required by the electrolyzer is supplied directly by the photovoltaic field.

In addition, the annual hydrogen demand is covered a half directly by the electrolyzer production and the other half by the gas contained in the tank.

Moreover, considering selling the excess electricity produced by the photovoltaic panels, the hydrogen cost decreases to **8.70 €/kg**.

Finally, the levelized cost of hydrogen for the latter sizing of the production plant has been assessed assuming a future scenario. Considering that the electrolyzer 2030 cost target is met, and that the electrolyzer efficiency is significantly improved, reaching the 2050 target value, the levelized cost of hydrogen would take the value of **8.71 €/kg** (selling the excess PV energy: 6.39 €/kg).

4.7   Preliminary conclusions

Specific components sizes have been found which allow to totally satisfy the hydrogen demand all year and to reduce as much as possible the levelized cost of hydrogen, which has been obtained equal to 15.02 €/kg$_{H2}$.

The photovoltaic field must have a peak power of 9.5 MWp, which corresponds to a land use of around 23 ha. A large PV plant is needed because the hydrogen is demanded also during the less sunny months and at an even higher flow rate. In particular, during the winter months of January and December, the request is 50% higher than that during the month of September.

The battery bank has been selected with a small capacity, equal to 795 kWh. It has been noted, indeed, that the component which more affects the overall cost is the battery.

The AEM electrolyzer is characterised by a rated power of 4995 kW, which corresponds to a nominal production rate of 79 kg/h (884 Nm3/h).

Finally, it has been chosen a hydrogen buffer able to store 4.995 tons of gas at 20 bar.

In the chosen system, considering a full year, 41% of the total photovoltaic power production is curtailed, because not used. However, being a large amount, it can be sold or used by the industrial plant itself. In this way, the LCOH is reduced.

Finally, since in the coming years a considerable increment of the AEM electrolyzer efficiency is expected, a system provided with a more efficient AEM electrolyzer has been sized, trying to minimize the levelized cost of hydrogen produced. It has been obtained that a smaller photovoltaic field, battery and electrolyzer are required to meet the year-round demand for hydrogen compared to the previous system. In particular, it has been observed that by increasing the electrolyzer efficiency by 20%, the required photovoltaic plant has a peak power's decrement of 2 MWp.

In addition, considering that the AEM electrolyzer starts to be used on a commercial scale, its investment cost will decrease a lot. Considering these future assumptions, the LCOH will decrease by around 6.3 €/kg$_{H2}$.

Because the industrial plant is located in an area with the possibility of a grid power connection, it is reasonable assuming a grid-connected hydrogen-producing system.

Therefore, in the next chapter, two new possible configurations will be analysed, wherein in each one, only the electrolyzer power supply will be modified: photovoltaic power supply with grid support and feed totally from the grid.

Finally, the previously investigated system and the new ones will be compared to determine the most economically convenient.

4.8 Scenarios' comparison

Considering having the possibility of connection to the power grid, two different configurations of hydrogen producing units have been modelled.

In the two systems, only the electrolyzer power supply differs: in one case the electrolysis unit is fed by power coming from a photovoltaic field and, when necessary, from the grid; in the other case the electrolyzer is grid-connected.

The configuration with both the photovoltaic field and the electrical grid is represented in Figure 42.
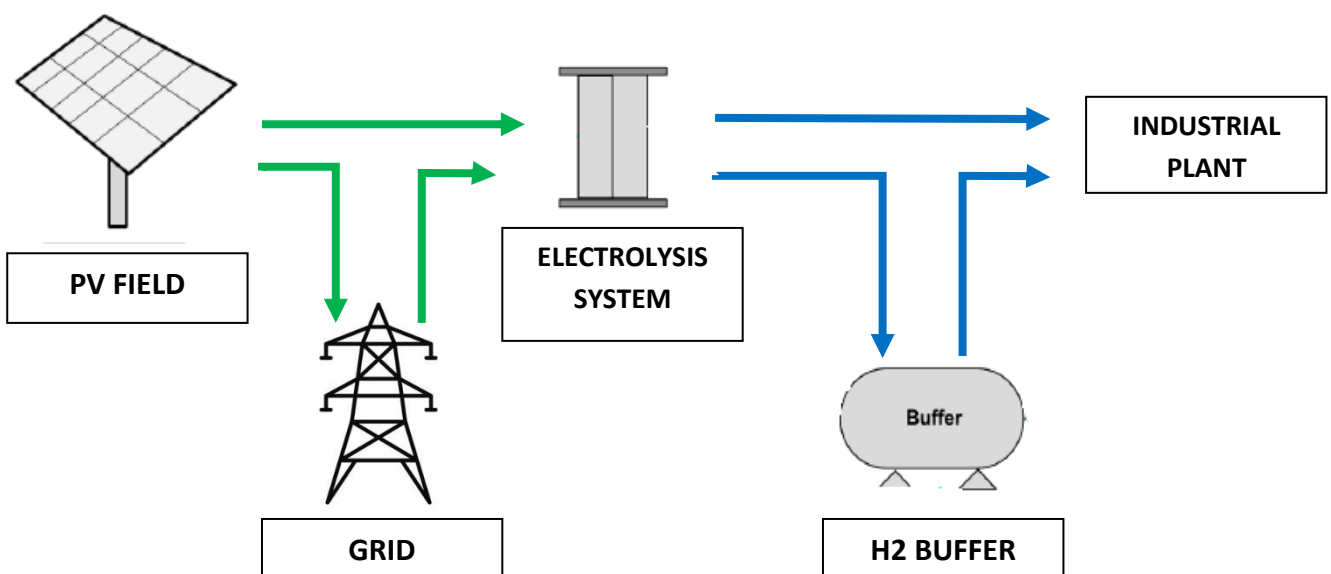
*Figure 42 – Layout of the configuration with both PV field and power grid support*

In this system the battery bank is not installed, and the electrolyzer is connected to both the PV plant and the electric grid.

Whenever the PV power production doesn't satisfy the hourly energy demand, the grid compensates it providing energy. Therefore, the grid acts as a "balancing entity", substituting the battery.

Instead, Figure 43 shows the system where both the PV field and the battery bank are not installed, and the electrolyzer is grid-connected.
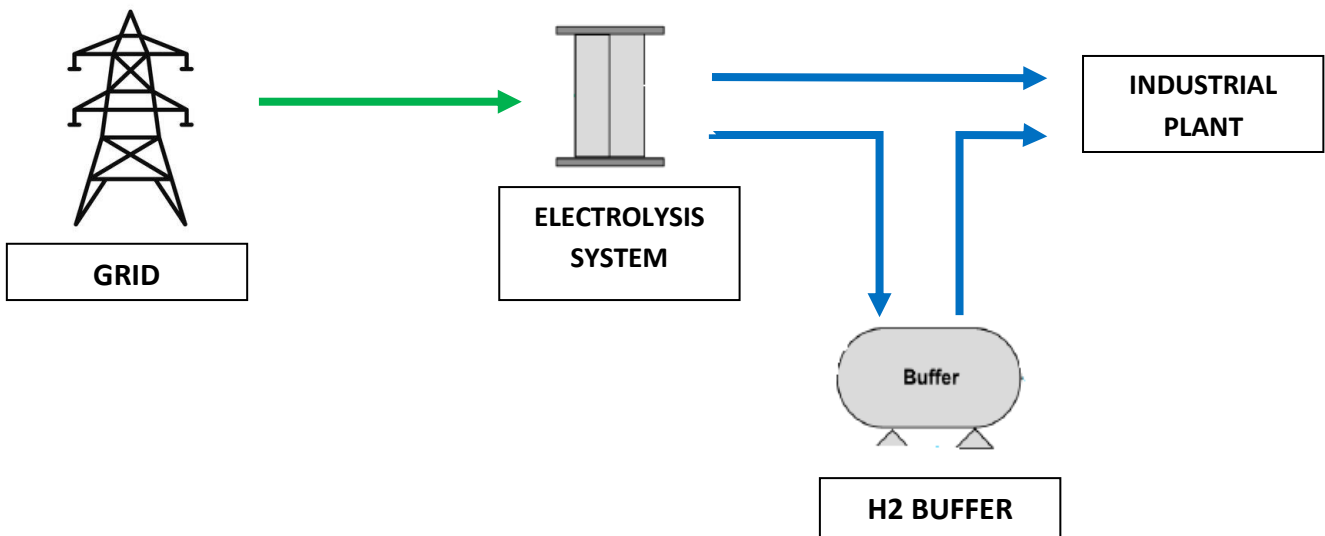
Figure 43 – Layout of the grid-connected configuration

In both these systems, it is still necessary the hydrogen buffer. In fact, when the hydrogen demanded by the industrial plant is greater than the maximum production rate of the electrolyzer or smaller than its minimum production capacity, the buffer must intervene to satisfy the demand.

Furthermore, hydrogen storage must always be present to meet the request in case of failure of the production system.

Regarding the simulation, all the assumptions of the previous case have been made and in addition, it has been assumed that the power grid is able to supply immediately all the required energy and to store all the not used energy.

Furthermore, the same criteria of the off-grid case have been followed with only the following modifications:

- Scenario with PV field and grid. Instead of demanding energy to the battery, it is supplied by the grid. Therefore, the needed energy is always available.
- Scenario without PV, grid connected. All requested energy is always and totally supplied by the grid.

Concerning the economic analysis, all the assumptions previously made have been kept.

It is assumed that the industry would contract a power purchase agreement to procure only renewable electricity [34]. Therefore, the produced hydrogen can be classified as green hydrogen anyway.

In Italy the electricity price is not constant, but it changes both during the day and with the amount of purchased electricity [29]. Taking into account this variability and considering an annual electricity

consumption of the plant lower than 5 GWh/year, it has been assumed an average price of electricity equal to 109 €/MWh [29].

4.8.1 Results

In Table 20 the sizes of the components of the three systems are shown. These are the sizes that guarantee to satisfy the hydrogen demand all hours of the year and to obtain the lowest possible levelized cost of hydrogen, for each configuration.

	PV field	Battery bank	Electrolysis unit	H2 buffer
Scenario 1: PV + battery + electrolyzer + H2 buffer	9.5 MWp	795 kWh	4995 kW	4.995 ton
Scenario 2: PV + grid + electrolyzer + H2 buffer	1.3 MWp	/	755 kW	0.505 ton
Scenario 3: Grid + electrolyzer + H2 buffer	/	/	770 kW	0.175 ton

Table 20 – Components sizes in the 3 scenarios

As it can be noted, because of the grid support, in the two new scenarios the components are much smaller compared to the off-grid ones.

Both scenarios 2 and 3 are provided with an electrolyzer of rated power around 800 kW and of a hydrogen buffer in the range of hundreds of kilograms.

The photovoltaic field required when there is the possibility of grid connection is much smaller than what is required in an off-grid application. However, to minimize the LCOH, it still has to have a quite big dimension of 1.3 MWp.

Table 21 reports and compares the main technical characteristics of the three scenarios.

	Scenario 1	Scenario 2	Scenario 3
PV power curtailment	41.3 %	17.2%	/
Electrolyzer capacity factor	37.5%	96.1%	95.5%
Power requested covered by PV	100%	21.9%	/
Power requested covered by grid	/	78.1%	100%
Hydrogen demand directly covered by electrolyzer production	48.9%	68.6%	69.9%
Hydrogen demand covered by buffer	51.1%	31.4%	30.1%

Table 21 – Main parameters of the 3 scenarios

As it can be observed, the PV power curtailment is much reduced in scenario 2. In fact, the system with grid support doesn't need a so big photovoltaic plant as in the previous case to satisfy the energy required by the electrolyzer, because whenever the available PV energy doesn't meet the demanded one, the grid provides what lacking. However, the power curtailment is not equal to zero, because even though for few hours, it happens that the photovoltaic energy is greater than the demanded one. This surplus electricity can be sold to the power grid or used for other purposes.

Furthermore, in scenario 2, the PV field is able to cover only 22% of the energy requested by the electrolysis unit. Around 78% of the energy is, indeed, supplied by the grid.

Differently from scenario 1, where around one half of the hydrogen demand is covered directly by the electrolyzer production and the other half by the hydrogen stored into the buffer, in both the other 2 scenarios, as expected, almost 70% of the total demand is provided directly by the electrolyzer. The electrolyzer, indeed, produces most of the time exactly what is required, because it is always provided with the needed energy.

However, the percentage of hydrogen provided by the buffer is not zero, because some hydrogen has to be taken from the tank when the demand is smaller than the minimum production of the electrolyzer or it's greater than its maximum production.

Regarding the electrolyzer capacity factor, those of the last two configurations are very high. Being the electrolyzer sizes smaller than the one of system 1, indeed, they work much more time at their rated conditions.

Finally, the levelized costs of hydrogen of the three systems are compared in Table 22.
Both the hydrogen cost considering curtailing the surplus PV energy and the hydrogen cost considering selling to the power grid the surplus PV energy, at the price of 50 €/MWh, have been computed.
In both these cases, the cheapest configuration is represented by scenario 2, where the electrolyzer is supplied by a photovoltaic field with a grid support. Instead, the most expensive system is the off-grid configuration.

	Scenario 1	Scenario 2	Scenario 3
LCOH (without selling the curtailed PV power)	15.02 €/kg$_{H2}$	7.38 €/kg$_{H2}$	7.90 €/kg$_{H2}$
LCOH (selling the curtailed PV power)	12.51 €/kg$_{H2}$	7.24 €/kg$_{H2}$	7.90 €/kg$_{H2}$

Table 22 – LCOHs of the three scenarios

Considering selling the surplus electricity, the costs of scenarios 1 and 2 decrease. In particular, the first decreases more because the surplus energy is much higher in the first system (41%) than in the second one (17%).
Of course, in scenario 3 there is not any change because it is not equipped with a PV field.

Figure 45 and Figure 44 show the breakdown of the overall cost of the configuration with PV field and grid support and that of only grid connection.
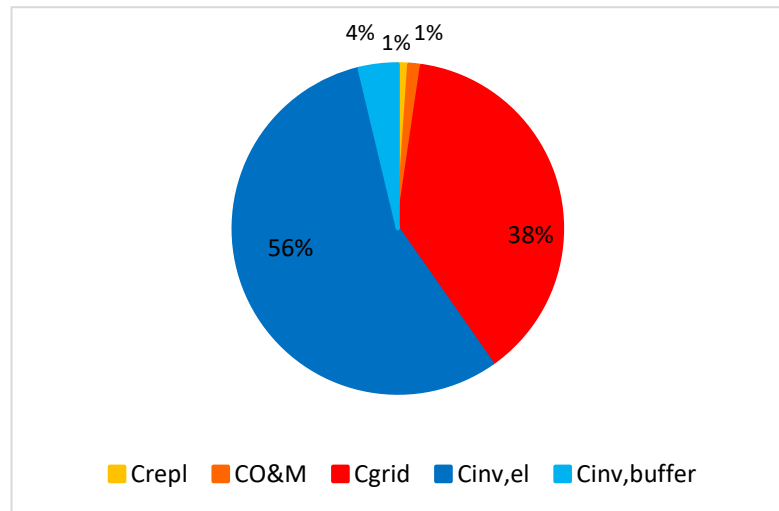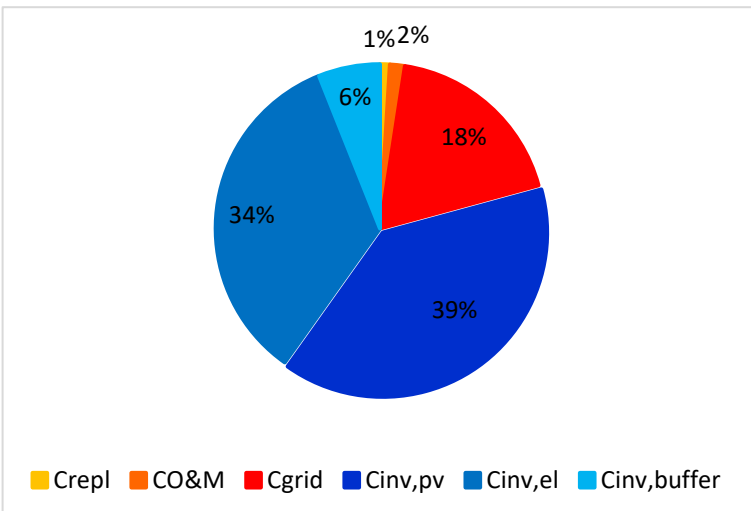

*Figure 45 – Breaking down of the overall cost – scenario 2*

Figure 44 – Breaking down of the overall cost – scenario 3

In both cases, the investment cost is responsible of around 60% of the overall cost.

In scenario 2, in particular, the high investment cost is due to the PV field and electrolyzer costs, while in scenario 3 the main cost is that of the electrolyzer.

The purchasing cost of electricity from the grid represents only 18% in system 2, while a higher amount in system 3, 38%.

4.8.2 Sensitivity analysis

Since the electricity price fluctuates a lot and it changes every year, a sensitivity analysis on the LCOH has been carried out. Figure 46 shows the variation of the hydrogen cost changing the electricity price.

As expected, as the price of electricity increases, the LCOH of the two configurations connected to the grid increases as well and it becomes increasingly more convenient to power the electrolyzer not only from the grid but also from a photovoltaic field. In fact, when the electricity price is equal to 90€/MWh, the LCOHs obtained in scenarios 2 and 3 differ by only 0.3 €/MWh, while increasing the electricity price at 120 €/MWh they differ by almost 1 €/MWh.

Furthermore, as it can be noted, for all electricity prices the most profitable solution is to connect the electrolyzer to both the PV field and the power grid. However, as the electricity price increases, to keep the hydrogen cost low, a larger photovoltaic field must be installed and therefore a higher percentage of the energy demand will be covered by the photovoltaic production.

Instead, avoiding the installation of a photovoltaic field and powering the electrolyzer only with energy coming from the grid is more profitable than the off-grid configuration until purchasing power from the grid costs less than 190 €/MWh. After that, producing hydrogen with an off-grid system becomes more convenient.
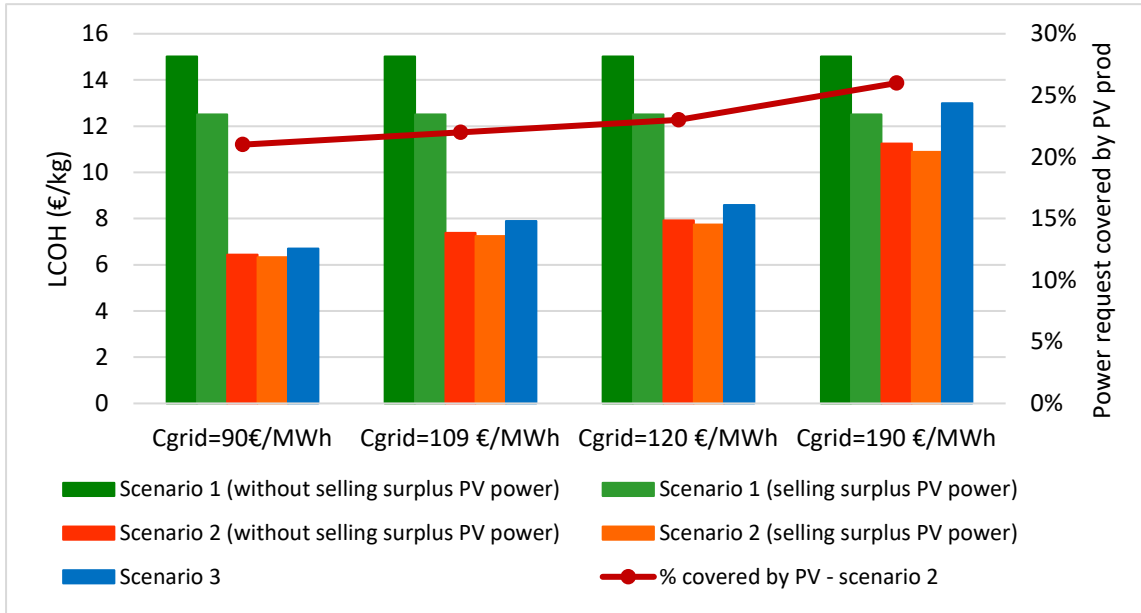

Figure 46 – LCOH variation with electricity price increment

Therefore, the more the electricity price increases, the higher will be the percentage of the energy required by the electrolyzer which is covered by the photovoltaic field production, until the most cost-effective system configuration achievable will result be the off-grid one.

4.9   Final considerations

The industrial plant requires hydrogen at a high and almost constant flow rate all the year. Therefore, to fulfil this requirement, considering not having the possibility of connection to the grid, a very big photovoltaic field is needed. A very large land thus has to be available and further costs related to a possible land rent should be added.

The levelized cost of hydrogen produced from this stand-alone system is around **15 €/kg$_{H2}$** and it has been obtained by reducing as much as possible the size of the battery bank, since it's the most expensive component and it most affects the overall cost.
It has been calculated that in a future scenario, where the AEM electrolyzer investment cost decreases and its efficiency increases up to the 2030 FCH JU target value, the hydrogen cost would reduce to 8.71 €/kg$_{H2}$.

However, if the grid power connection is possible, it's more convenient to build a smaller photovoltaic field and use the power grid in place of an-onsite storage system. With this configuration the LCOH has turned out equal **7.38 €/kg$_{H2}$**.
It has been observed that supply the electrolyzer only with energy coming from the grid is less convenient.
Furthermore, another advantage of having a PV plant is that, especially during the summer months, it produces surplus electricity, which is not used to produce hydrogen. All excess energy can be used by the same industrial plant for other purposes or can be sold, thus allowing further revenues.
Moreover, it has been observed that as the electricity price increases, it's more convenient building a larger photovoltaic field and reducing the amount of energy taken from the power grid, and thus increasing the feeding of the electrolyzer by the PV field and reducing that by the grid.

In addition, it has been noted that, if it hadn't been for the high hydrogen demand and low solar power availability during the period of December-January, a smaller photovoltaic field would have been needed. Therefore, the electrolyzer could be connected to the power grid during these months and connected to a smaller PV field and battery during the remaining ones.
This solution should be deeply investigated, however the presence of the battery leads to think that the LCOH could be higher than in the configuration without the battery.

5   Conclusions

As regards the assessment of the pre-commercial AEM electrolyzer, despite the high variability of the test data because of experimental limitations, some confident results have been obtained and the following conclusions can be drawn.

The stack efficiency has resulted much lower than expected: at a current density of 0.4 A/cm2 and hydrogen production pressure of 1 bar and 20 bar, the efficiency reached the value of 58.8% and 55.6%, respectively. The main reason for this low performance is the mismatch between theoretical hydrogen production and real production. This is due to phenomena happening at both stack level and overall system level. Furthermore, it has been noted that the electrolysis efficiency varies a lot depending on the flow rate of hydrogen produced. In particular, it decreases passing from rated hydrogen production to low production. As well as with the production level, the electrolyzer performance varies with both operating temperature and hydrogen production pressure. It has been observed that the cell temperature is more impacting on the efficiency than the pressure. For this reason, a proposal to improve the performance of the electrolyzer is to integrate a thermoregulation system to stabilize the temperature at a value that allows maximum efficiency to be reached in all operating conditions.

Instead, in the second section of the thesis, a power-to-hydrogen system has been modelled to feed an industrial plant's cogeneration unit.

In the first place, it has been considered an off-grid plant composed of a photovoltaic field, a battery bank, the AEM electrolyzer, and a hydrogen buffer.
However, mainly because of the hydrogen request, which is greater in the winter months than in the summer periods, and secondarily because of the electrolyzer's low efficiency, a large PV field of peak power equal to 9.5 MWp is required.
Then, it has been simulated the case of having an electrolyzer characterized by a system efficiency equal to the 2050 FCH JU target. A reduction in the size of all components has been observed. In particular, increasing the electrolyzer efficiency to 74%, the required PV field size lowered by 2 MWp.

Finally, since the site, where the industrial plant is located, has the possibility of grid power connection, two further hydrogen-producing systems have been analysed: the former is provided with electrolyzer power supply coming from both the grid and the PV field, while the latter with power supplied totally from the grid. For this specific hydrogen demand, solar availability, actual characteristics of the electrolyzer and selected electricity price, both are resulted more profitable than the off-grid configuration, from an economic point of view.

For the first one, especially, the lowest LCOH (7.38 €/kgH2) has been obtained. The configuration consists of a photovoltaic field of 1.3 MWp, an AEM electrolyzer of rated power equal to 755 kW, and a buffer capable of store 505 kg of hydrogen.

Concluding, considering the actual electrolyzer technology level and the yearly trend of the hydrogen requested by the industrial plant, the off-grid configuration is not economically the best, and, on the contrary, the system provided with a PV field and the connection to the power grid has turned out as the more adequate scenario.

6 References

[1] SNAM, "The hydrogen challenge: the potential of hydrogen in Italy," 2019.

[2] I. R. E. Agency, "Innovation landscape brief: renewable poer to hydrogen," 2019.

[3] L. Kouchachvili and E. Entchev, "Power to gas and H2/NG blending in SMART energy networks concept," *Elsevier,* 2018.

[4] Miller, Bouzek, Hnat, Loos and Bernacker, "Green hydrogen from anion exchange membrane: a review of recent developments in critical materials and operating conditions," *Sustainable energy fuels,* 2020.

[5] I. R. E. Agency, "Hydrogen from renewable power: technology outlook for the energy transition," 2019.

[6] I. Vincent and D. Bessarabov, "Low cost hydrogen production by AEM electrolysis: A review," *ELSEVIER,* 2017.

[7] K. Ayers, N. Danilovic, R. Ouimet, M. Carmo, B. Pivovar and M. Bornstein, "Perspectives on low-temperature electrolysis and potential for renewable hydroen at scale," *Annual review of chemical and biomolecular engineering,* 2019.

[8] E. e. &. r. energy. [Online]. Available: https://www.energy.gov/eere/fuelcells/hydrogen-production-electrolysis.

[9] J. Brauns and T. Turek, "Alkaline water electrolysis powered by renewable energy: a review," *MDPI,* 2020.

[10] S. Shiva Kumar and V. Himabindu, "Hydrogen production by PEM water electrolysis – A review," *Elsevier,* 2019.

[11] Enapter, 2020. [Online]. Available: https://www.enapter.com/it/aem-water-electrolysis-how-it-works.

[12] M. Bos, S. Kersten and D. Brilman, "Wind power to methanol: renewable methanol production using electricity, electrolysis of water and CO2 air capture," *Elsevier,* 2020.

[13] I. I. Inc, "Hydrogen production cost by AEM water electrolysis," 2020.

[14] R. Edison, "H2 by water electrolysis - KPIs comparison," 2020.

[15] A. Buttler and H. Spliethoff, "Current status of water electrolysis for energy storage, grid balancing and sector coupling via power-to-gas and power-to-liquids: A review," *Elsevier,* 2017.

[16] I. E. Agency, "The future of hydrogen - seizing today's opportunities," 2019.

[17] M. Lappalainen, "Techno-economic feasibility of hydrogen production via polymer membrane electrolyte for future power-to-x systems," Tampere University, 2019.

[18] A. Buttler and S. Hartmut, "Current status of water electrolysis for energy storage, grid balancing and sector coupling via power-to-gas and power-to-liquids: A review," *Renewable and Sustainable Energy Reviews,* 2017.

[19] "Equilibar," [Online]. Available: https://www.equilibar.com/back-pressure-regulators/how-it-works/bpr-definition/.

[20] H. Ito, N. Kawaguchi, S. Someya and T. Munakata, "Pressurized operation of anion exchange membrane water electrolysis," *Elsevier,* 2018.

[21] H. Ito, N. Kawaguchi, S. Someya, T. Munakata, N. Miyazaki, M. Ishida and A. Nakano, "Experimental investigation of electrolytic solution for anion exchange membrane water electrolysis," *Elsevier,* 2018.

[22] A. Awasthi, K. Scott and S. Basu, "Dynamic modeling and simulation of a proton exchange membrane electrolyzer for hydrogen production," *Elsevier,* 2011.

[23] D. Jang, H. Cho and S. Kang, "Numerical modeling and analysis of the effect of pressure on the performance of an alkaline water electrolysis system," *Elsevier,* 2021.

[24] IRENA, "Green hydrogen cost reduction: scaling up electrolysers to meet the 1.5°C climate goal," 2020.

[25] P. Marocco, D. Ferrero, M. Gandiglio, M. Ortiz, K. Sundseth, A. Lanzini and M. Santarelli, "A study of the techno-economic feasibility of H2-based energy storage systems in remote areas," *Elsevier,* 2020.

[26] D. Ipsakis, S. Voutetakis, P. Seferlis, F. Stergiopoulos and S. Papadopoulou, "The effect of the hysteresis band on power managaement strategies in a stand-alone power system," *Elsevier,* 2008.

[27] P. Marocco, D. Ferrero, M. Gandiglio and M. Santarelli, "REMOTE - Technical specification of the technological demonstrator," 2018.

[28] marcogaz, "Overview of available test results and regulatory limits for hydrogen admission into existing natural gas infrastructure and end use," 2019.

[29] M. Minutillo, A. Perna, A. Forcina, S. Di Micco and E. Janelli, "Analyzing the levelized cost of hydrogen in refueling stations with on-site hydrogen production via water electrolysis in the Italian scenario," *Elsevier,* 2020.

[30] J. Yates, R. Daiyan, R. Patterson, R. Egan, R. Amal, A. Ho-Baille and N. Chang, "Techno-economic analysis of hydrogen electrolysis from off-grid stand-alone photovoltaics incorporating uncertainty analysis," *Cell Reports Physical Science,* 2020.

[31] L. Gracia, P. Casero, C. Bourasseau and A. Chabert, "Use of hydrogen in off-grid locations, a techno-economic assessment," *MDPI - energies,* 2018.

[32] T. E. S. a. Hinicio, "Study on early business cases for H2 in energy storage and more broadly power to H2 applications," 2017.

[33] Market observatory for energy of the european comm, "Quarterly Report on European Electricity Markets with focus on corporate power purchase agreements and residential photovoltaics," 2019.

[34] A. C. -. ICCT, "Assessment of hydrogen production costs from electrolysis: United States and Europe," 2020.

[35] J. Rodriguez, J. Oviedo and E. Amores, "Development of an operation strategy for hydrogen production using solar PV energy based on fluid dynamic aspects," *Researchgate,* 2017.